Research Paper

# Identification of AhR agonists in sediments of the Bohai and Yellow Seas using advanced effect-directed analysis and in silico prediction

Junghyun Lee [a], Seongjin Hong [b,*], Taewoo Kim [a], Shin Yeong Park [a], Jihyun Cha [b], Youngnam Kim [b], Jiyun Gwak [b], Sunggyu Lee [c], Hyo-Bang Moon [c], Wenyou Hu [d], Tieyu Wang [e], John P. Giesy [f,g], Jong Seong Khim [a,*]

[a] School of Earth and Environmental Sciences & Research Institute of Oceanography, Seoul National University, Seoul 08826, Republic of Korea
[b] Department of Marine Environmental Science, Chungnam National University, Daejeon 34134, Republic of Korea
[c] Department of Marine Science and Convergence Engineering, Hanyang University, Ansan 15588, Republic of Korea
[d] Key Laboratory of Soil Environment and Pollution Remediation, Institute of Soil Science, Chinese Academy of Sciences, Nanjing, China
[e] Institute of Marine Sciences, Shantou University, Shantou 515063, China
[f] Department of Veterinary Biomedical Sciences & Toxicology Centre, University of Saskatchewan, Saskatoon, Saskatchewan S7N5B3, Canada
[g] Department of Environmental Science, Baylor University, Waco, TX 76798-7266, United States

## HIGHLIGHTS

- AhR potencies in sediments from the Yellow and Bohai Seas at large scale were evaluated.
- Unmonitored AhR-active compounds in sediments identified using advanced EDA.
- DBcP and IcdF were identified as novel AhR agonists in sediments.
- Assay-specific relative potency values were obtained for dominant AhR agonists.

## GRAPHICAL ABSTRACT
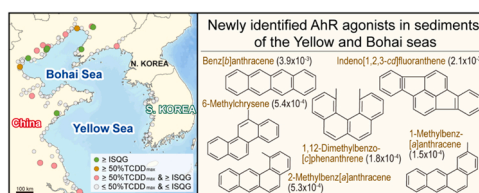


## ARTICLE INFO

Editor: Karina S.B. Miglioranza

## ABSTRACT

Novel aryl hydrocarbon receptor (AhR) agonists were identified in coastal sediments in the Yellow and Bohai Seas by use of a combination of effect-directed analysis (EDA) and in silico prediction. A total of 125 sediments were screened for AhR-mediated potencies using H4IIE-*luc* bioassay. Great potencies were observed in organic extracts, mid-polar fraction (F2), and subfractions of F2 (F2.6–F2.9) of sediments collected from Nantong, Qinhuangdao, and Yancheng. Less than 15% AhR potencies could be explained by detected dioxin-like PAHs. Full-scan screening analysis was conducted for the more potent fractions using GC-QTOFMS to investigate the presence of unmonitored AhR agonists. A five-step prioritization strategy was applied; 92 candidate compounds satisfied all criteria. Among these chemicals, thirteen were evaluated for AhR efficacy. Six compounds; benz[*b*]anthracene, 6-methylchrysene, 2-methylbenz[*a*]anthracene, 1-methylbenz[*a*]anthracene, 1,12-dimethylbenzo[*c*]phenanthrene, and indeno[1,2,3-*cd*]fluoranthene, exhibited significant AhR-mediated efficacies. 1,12-dimethylbenzo[*c*]phenanthrene and indeno[1,2,3-*cd*]fluoranthene were identified as novel AhR agonists. Potency balance analysis showed that the six newly identified AhR agonists explained 0.4–100% of the total AhR-mediated potencies determined. Overall, combining EDA and in silico prediction applied in this study demonstrated the benefits of assessing the potential toxic effects of previously unidentified AhR agonists in sediments from the coasts of China and Korea.

* Corresponding authors.
   E-mail addresses: hongseongjin@cnu.ac.kr (S. Hong), jskocean@snu.ac.kr (J.S. Khim).

## 1. Introduction

Sediments of estuaries, harbors, and coastal areas are known to serve as sinks of contaminants and represent risks to both environments and humans who consume seafood from those areas (Hollert et al., 2003; Bláha et al., 2006). Rapid industrialization and urbanization have occurred in the coastal areas of South Korea and China, which adjoin the Yellow and Bohai Seas, resulting in contamination of sediments (Meng et al., 2017; Khim et al., 2018). Our research group previously found that various toxic substances are widely distributed in sediments of the Yellow and Bohai Seas, including alkylphenols, styrene oligomers, organochlorines, perfluorinated compounds, pharmaceuticals, personal care products, and metals (Meng et al., 2017; Tian et al., 2020; Yang et al., 2020; Yoon et al., 2020). Of note, in some hot spot areas, concentrations of dioxin-like chemicals (DLCs) were identified and quantified on a scale that causes endocrine disruption in aquatic organisms after long-term exposure (Denison and Nagy, 2003).

The presence of DLCs in sediment is a constant environmental issue, because they have a variety of toxic effects, including mutagenic, teratogenic, and carcinogenic in animals and humans with serious health concerns (Wang et al., 2017). These chemicals include polycyclic aromatic hydrocarbons (PAHs), polychlorinated biphenyls (PCBs), polychlorinated dibenzo-*p*-dioxins, and furans (PCDD/Fs), all of which to one degree or another can activate aryl hydrocarbon receptor (AhR)--mediated pathways. However, monitoring have only focused on the occurrence of DLCs, and studies on the potential toxic effects of contaminated sediments in these regions have been limited (Hwang et al., 2021). Thus, more efforts are urgently required to monitor and identify DLCs by integrating chemical analysis and bioassays.

Assessments of risks posed by DLCs in sediments are complicated because these compounds occur as complex mixtures with varying persistence, accumulation, and degradability (Giesy et al., 2002). Although extensive chemical analyses have been performed, this approach provides insufficient information on compounds for which authentic standards are not available and/or when analytical methods have not been developed. In addition, this approach does not account for integrated biological potency by possible interactions between or among individual chemicals, such as additive, synergistic, or antagonistic effects (Chapman, 2007). To improve the strategy of environmental monitoring and assessment, a combination of bioassays and in silico prediction, and high-resolution mass spectrometry have been employed to characterize and predict the combined toxic effects of pollutants in sediments (Xiao et al., 2016).

The H4IIE-*luc* in vitro transactivation bioassay has been used to assess the potential AhR efficacy of DLCs in environmental complex mixtures, including those in sediment (Hong et al., 2014; Larsson et al., 2014a; Lee et al., 2017). Through this approach, the bioassay-derived 2,3,7,8-tetrachlorodibenzo-*p*-dioxin (TCDD) equivalent concentrations (EQs) in organic extracts of sediments can be determined and directly compared with instrument-derived TCDD equivalent concentrations (TEQs) (Hong et al., 2014; Larsson et al., 2014a). Comparison of TCDD-EQs and TEQs through the use of potency balance analysis is useful for understanding the total concentrations of AhR agonists in extracts and relative contributions of monitored and previously unmonitored DLCs in samples. Unexplained AhR-mediated potencies in sediments indicate the occurrence of mixture interactions and/or the presence of previously unidentified and uncharacterized AhR agonists (Lee et al., 2017, 2018).

The toxic potencies of compounds for which no standards are available and unknown could be predicted using in silico techniques. This approach also has the advantage of saving time and resources spent on the experimental toxicity assessment (Muster et al., 2008). Quantitative structure-activity relationships (QSAR) modeling represents a process in which chemical structures are quantitatively correlated with biological activities. When analyzed by QSAR, chemicals with the same or similar molecular formulae might exhibit similar efficacies and potencies for a common endpoint, or might be very different depending on the positions of moieties in isomers. To complement this limitation, the automated program VirtualToxlab combines multi-dimensional QSAR and flexible docking was used (Vedani et al., 2012). Molecular docking is an analytical approach to predict the compatibility of the binding site of receptors to specific chemical groups by computing the most favorable receptor-chemical binding configuration with minimal potential energy (Vedani et al., 2015).

By combining effect-directed analysis (EDA) and full-scan screening analysis (FSA) is possible to identify causative chemicals in sediments (Hecker and Giesy, 2011). EDA is the approach that combines in vitro/in vivo bioassays with multi-step fractionation in order to reduce the complexity of chemical mixtures and chemical analysis of bioactive fractions (Brack, 2003; Hong et al., 2016a). FSA with high-resolution mass spectrometry (HRMS) represents a feasible technique for detecting and identifying emerging contaminants based on accurate measurements of molecular mass (Hernández et al., 2015). It was proved to be an efficient analytical tool for the rapid screening and confirmation of a large number of non-target compounds (Zhang et al., 2014). 'Screening' means a single tool applied to identify and check all peaks corresponding to compounds in sediments (Schymanski et al., 2015). Some novel AhR agonists in sediments have been identified successfully using this approach (Cha et al., 2019; Lee et al., 2020; Gwak et al., 2022).

The objectives of this study were to investigate the potential efficacy and potency mediated through AhR in sediments collected on a large scale from coastal areas of the Yellow and Bohai Seas, and to identify previously unmonitored AhR agonists using advanced EDA combined with in silico prediction. Once previously unknown compounds were tentatively screened using gas chromatography with a quadrupole time-of-flight mass spectrometry (GC-QTOFMS). To increase the identification confidence of AhR-active candidate compounds, once identified these compounds were prioritized, to be further characterized by determining their relative effect potency (ReP) as AhR agonists in the H4IIE-*luc* transactivation assay. In addition, in silico modeling was applied to predict the potential toxicities of AhR agonist candidates. Finally, relative contributions of newly identified AhR agonists to overall induced AhR-mediated potencies were assessed using potency balance approaches.

## 2. Materials and methods

### 2.1. Sampling and sample preparation

An overview of workflow of the study was presented in Fig. 1. A set of sediment samples collected from a previous study were used in this study. Detailed information on sampling sites is provided in Yoon et al. (2020). All samples were collected in June–July 2018 along the coasts of the Yellow and Bohai Seas, including major rivers and estuaries. Surface sediments ($n = 125$) were collected at 0–3 cm depth using stainless steel devices (Fig. S1 of the Supplementary Materials). Samples were contained in pre-cleaned glass bottles and transported on dry ice to the laboratory. Samples were freeze-dried, homogenized with a mortar and pestle, and stored at − 20 ℃ until analysis.

### 2.2. Extraction and fractionation

Extractions and fractionations were performed as described previously, with minor modifications (Hong et al., 2015, 2016b). In brief, 30 g sediment was Soxhlet extracted for 16 h with 300 mL dichloromethane (DCM, Burdick & Jackson, Muskegon, MI). Elemental sulfur in organic extracts was removed by activated copper. Raw organic extracts (REs) were concentrated to approximately 5 mL using rotary evaporation, and volume was adjusted to 3 mL in hexane using a nitrogen gas concentrator (10 g sediment equivalent [SEq] mL$^{-1}$).

REs were fractionated in two steps (Fig. 1), namely, silica gel column

chromatography (8 g activated silica gel, 70–230 mesh, Sigma-Aldrich, Saint Louis, MO) and reverse-phase high-performance liquid chromatography (RP-HPLC, Agilent 1260 HPLC, Agilent Technologies, Santa Clara, CA) (for details, see Hong et al., 2015, 2016b). In brief, 3 mL REs were passed through silica gel column and separated according to polarity: non-polar (F1), mid-polar (F2), and polar (F3) fractions. The F1 was collected by the elution of 30 mL hexane. The F2 was eluted with 60 mL of 20% DCM in hexane, and 50 mL of 40% acetone in DCM was used to elute F3. The F2 fraction, which contained the DL-PAHs, was separated into 10 subfractions by use of RP-HPLC. Detailed instrumental conditions were previously reported (Hong et al., 2016b), and summarized in Table S1. The portion of the fraction to be used in bioassay was exchanged to dimethyl sulfoxide (DMSO).

### 2.3. In vitro H4IIE-luc bioassay

To assess AhR activation potential of REs, silica gel fractions, and RP-HPLC fractions, we used a recombinant cell-based bioassay, following established methods (Hong et al., 2016b). Rat hepatoma cells stably transfected with an AhR-luciferase reporter (H4IIE-*luc* cell line) were seeded in 96-well plates at a concentration of approximately 70,000 cells mL$^{-1}$ and incubated for 24 h (Table S2) at 37 °C in a 5% CO$_2$. Then, the plates were dosed with TCDD as a positive control, the prepared samples, and solvent control (0.1% DMSO). Luciferase assays were performed after 4 h and 72 h of exposure. The results were measured by mean luciferase luminescence (RLUs) using a microplate reading luminometer (PerkinElmer, Waltham, MA). Final luminescence values were expressed as adjusted RLU and mean solvent control response was subtracted from that of each sample, and percentages of the maximal response of TCDD were observed for 729 pM (=100%TCDD$_{max}$). Significant levels were calculated as those that were three times the standard deviation (SD) of the mean of the solvent controls. Potency-based TCDD-equivalent (EQ) concentrations (pg TCDD-EQ g$^{-1}$ dry mass (dm)) were determined directly from sample dose-response relationships generated by testing samples at six levels of dilutions. All experiments have been repeated a minimum of three independent times, and the results shown are averages ± SD.

### 2.4. Targeted chemical analyses

Concentrations of 15 traditional PAHs (*t*-PAHs) in the sediment samples were obtained from Yoon et al. (2020), who evaluated samples at the same stations in the Yellow and Bohai Seas. Fifteen *t*-PAHs and newly identified AhR agonists (*n*-PAHs) in the RP-HPLC fraction samples were analyzed by previously described methods using an Agilent 7890B GC coupled to the mass-selective detector (MSD, 5977B model) (Cha et al., 2019). Further details of instrumental conditions are described in Table S3. And the full names and method detection limits (MDLs) for targeted PAHs are provided in Table S4. MDLs were calculated as standard deviations of standard materials × 3.707, and ranged from 1.1 to 15.1 ng g$^{-1}$ dm for *t*-PAHs and 0.92–8.27 ng g$^{-1}$ dm for *n*-PAHs (Table S4). For quality control, procedural blanks were analyzed concurrently to check for interfering peaks. The mean concentrations of PAHs in blank samples were below the MDLs. Mean recoveries of four surrogate standards for PAHs were generally acceptable, with an average of 87% (Table S3).

### 2.5. Full-scan screening analysis

The most AhR potent fractions were screened in full scan mode to identify novel AhR agonists by use of GC equipped with a QTOFMS (Table S5). AhR agonist candidates were nominated using a five-step process (for details, see Section 3.3). Thirteen of the tentative AhR agonists were commercially available (Sigma-Aldrich), including, 1-methylbenz[*a*]anthracene (1MBaA), 1-methylphenanthrene, 1,12-dimethylbenzo[*c*]phenanthrene (DBcP), 2-methylbenz[*a*]anthracene (2MbaA), 4-methylbenzophenone, 6-methylchrysene (6MC), 7 H-benzo [*c*]fluorene, 9 H-xanthene, 9,9-dimethylxanthene, 9,10-dimethylanthracene, benzo[*b*]anthracene (BbA), indeno[1,2,3-*cd*]fluoranthene (IcdF), and triptycene. The 13 candidates, AhR agonists, were screened for AhR-mediated potencies at 4 h and 72 h. An additional 4 h exposure test was performed because the RLU in the H4IIE-*luc* bioassays could vary significantly between two exposure durations (4 h and 72 h) due to metabolism. Based on results of a previous study, metabolically stable compounds, such as PCDD/Fs and coplanar-PCBs, are relatively stable during longer exposure, while metabolically labile compounds, such as PAHs, can be more easily degraded (Lee et al., 2013).

### 2.6. Calculation of the relative effect potency values

Of the 13 AhR agonist candidates, ReP values were calculated for compounds that exhibit considerable AhR-mediated efficacies and potencies of authentic standards. ReP values for four of these compounds had been previously reported as AhR agonists (Table 1). However, the
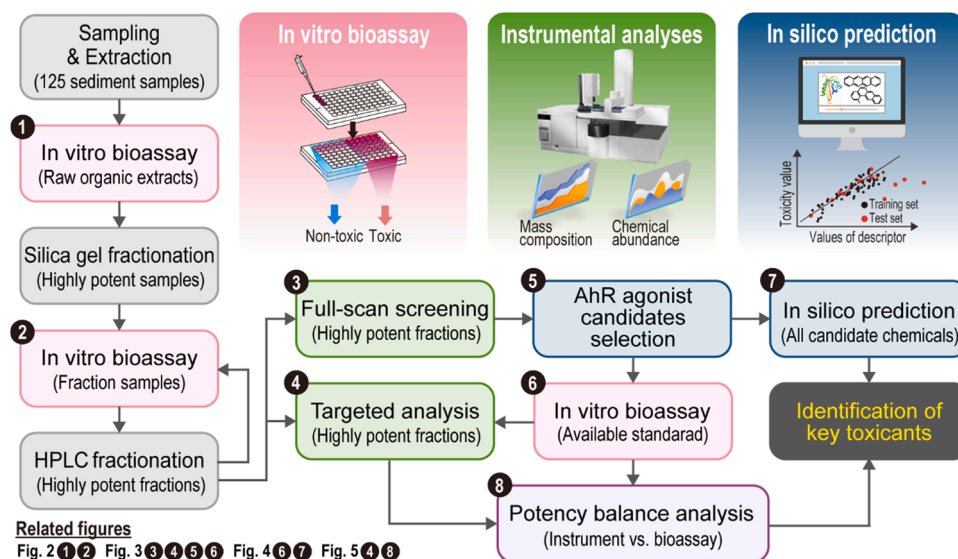


**Fig. 1.** Simplified flow diagram of the work carried out in the present study, including the bioassay, chemical analyses, and in silico prediction used to identify major AhR agonists in the sediments from the Yellow and Bohai Seas.

ReP values of all six compounds were newly estimated, because ReP values are assay- and exposure time-specific (Lee et al., 2013). Each compound was tested with a maximum concentration of 10,000 ng mL$^{-1}$ with following 5-point treatment series, prepared in serial 3-fold decrements, and was measured using the H4IIE-*luc* bioassay (72 h) method described in Section 2.3. ReP20, ReP50, and ReP80 of the compounds were estimated from the EC20, EC50, and EC80, respectively, of TCDD in the H4IIE-*luc* bioassay (Table S6). The use of ReP50 was considered reliable if the deviation between ReP20, ReP50, and ReP80 was within 10-fold (Horii et al., 2009). However, when the maximum efficiency did not reach 50%TCDD$_{max}$, the ReP20 value was used in the present study.

### 2.7. Potency balance analysis

To evaluate contributions of individual AhR agonists to total AhR efficacy, potency balance analysis was performed between bioassay-derived concentrations (TCDD-EQs) and instrument-derived concentrations (TEQs) (Table 2). Concentrations of TEQ of DL-PAHs were calculated from the sum of TEQs by multiplying the concentrations of individual DL-PAHs and their assay-specific ReP values. RePs of *t*-PAHs, including seven DL-PAHs were obtained from Villeneuve et al. (2002).

### 2.8. In silico prediction

Potential AhR binding affinities of tentative AhR agonist candidates, including chemicals for which standard chemicals were commercially unavailable, were predicted using VirtualToxLab (Vedani et al., 2015). The toxic potential (TP) is derived through the normalized individual binding affinity and weighted by use of the standard deviation of the individual prediction. TP is classified into seven groups: TP $\leq 0.3$ (None), $0.3 < $ TP $\leq 0.4$ (Low), $0.4 < $ TP $\leq 0.5$ (Moderate), $0.5 < $ TP $\leq 0.6$ (Elevated), $0.6 < $ TP $\leq 0.7$ (High), $0.7 < $ TP $\leq 0.8$ (Very high), and TP $> 0.8$ (Extreme) (Vedani et al., 2015). The smaller the value of binding affinity, the greater reaction between ligands and receptors occurs. In order to obtain an intuitive understanding of how potential toxicity increases with an increasing binding affinity, the inverse value of binding affinity was used.

## 3. Results and discussion

### 3.1. Screening of AhR-mediated potencies in raw extracts and fractions

Among the 125 samples of sediments, 117 induced significant AhR-mediated potencies ranging from 1.2% to 107%TCDD$_{max}$ (Fig. 2). The

**Table 1**

Characteristics and relative effect potency values (RePs) of AhR agonists in the RP-HPLC fractions (F2.6–F2.8) of sediment samples (QH6, YC6, and NT10) from the Yellow and Bohai Seas.

| Fraction/compound | Use/origin | Molecular formula | CAS number | MW[a] | Matching factor[b] | Cell line | Standard Chemical | Exposure time | RePs | References |
|---|---|---|---|---|---|---|---|---|---|---|
| *Fraction 2.6* | | | | | | | | | | |
| BbA | Film layer of OFETs& OLEDs[c] | $C_{18}H_{12}$ | 92–24–0 | 228.3 | 86 | H4IIE-*luc* | TCDD | 72 | $3.9 \times 10^{-3}$ | *This study* |
| | | | | | | | | 48 | $1.5 \times 10^{-5}$ | Larsson et al. (2014b) |
| | | | | | | | | 24 | $4.2 \times 10^{-4}$ | Larsson et al. (2014b) |
| | | | | | | | BaP | 4 | 10.6 | Cha et al. (2019) |
| | | | | | | YCM3 | BaP | -[d] | 35 | Murahashi et al. (2007) |
| | | | | | | RTL-W1 | BaP | – | $4.8 \times 10^{-1}$ | Bols et al. (1999) |
| | | | | | | | TCDD | – | $1.4 \times 10^{-4}$ | Bols et al. (1999) |
| *Fraction 2.7* | | | | | | | | | | |
| 6MC | Tobacco smoke[e] | $C_{19}H_{14}$ | 1705–85–7 | 242.3 | 85 | H4IIE-*luc* | TCDD | 72 | $5.4 \times 10^{-4}$ | *This study* |
| | | | | | | WB-F344 | TCDD | 24 | $1.2 \times 10^{-4}$ | Machala et al. (2008) |
| | | | | | | HepG2 | BaP | 24 | $7.9 \times 10^{-1}$ | Alqassim et al. (2019) |
| 2MBaA | Charcoal smokef | $C_{19}H_{14}$ | 2498–76–2 | 242.3 | 89 | H4IIE-*luc* | TCDD | 72 | $5.3 \times 10^{-4}$ | *This study* |
| | | | | | | WB-F344 | | 24 | $1.3 \times 10^{-4}$ | Marvanová et al. (2008) |
| 1MBaA | Smoky coal combustion[g] | $C_{19}H_{14}$ | 2498–77–3 | 242.3 | 72 | H4IIE-*luc* | TCDD | 72 | $1.5 \times 10^{-4h}$ | *This study* |
| | | | | | | WB-F344 | | 24 | $4.8 \times 10^{-5}$ | Marvanová et al. (2008) |
| DBcP* | – | $C_{20}H_{16}$ | 4076–43–1 | 256.3 | 81 | H4IIE-*luc* | TCDD | 72 | $1.8 \times 10^{-4\ h}$ | *This study* |
| *Fraction 2.8* | | | | | | | | | | |
| IcdF* | – | $C_{22}H_{12}$ | 193–43–1 | 276.3 | 94 | H4IIE-*luc* | TCDD | 72 | $2.1 \times 10^{-3}$ | *This study* |

*Newly identified AhR agonists.

[a] MW: Molecular weight.

[b] National Institute of Standards and Technology (NIST) library matching score (Ver. 2014).

[c] Takahashi et al. (2007)

[d] No information

[e] Hecht et al. (1974)

[f] Ré-Poppi and Santiago-Silva (2002)

[g] Mumford et al. (1995).

[h] ReP20 value was determined at the doses of a given chemical of which AhR responses are equivalent to 20% response levels of the maximum TCDD concentration in standard curves.

**Table 2**

Summary of the results for improved potency balance analysis between instrument-derived TEQs and bioassay-derived TCDD-EQs in the RP-HPLC fraction (F2.6–F2.8) of sediment samples (QH6, YC6, and NT10) from the Yellow and Bohai Seas.

| Target compounds | Abb[a] | QH6 | | | YC6 | | | NT10 | | |
|---|---|---|---|---|---|---|---|---|---|---|
| | | F2.6 | F2.7 | F2.8 | F2.6 | F2.7 | F2.8 | F2.6 | F2.7 | F2.8 |
| *Instrument-derived TEQs (pg TEQ g$^{-1}$ dm)* | | | | | | | | | | |
| **Traditional PAHs**[b] | | | | | | | | | | |
| Benzo[*a*]anthracene | BaA | 0.07 | | | 0.53 | | | 0.98 | | |
| Chrysene | Chr | 0.09 | | | 0.30 | | | 0.76 | | |
| Benzo[*b*]fluoranthene | BbF | | 0.34 | | | 3.08 | | | 5.43 | |
| Benzo[*k*]fluoranthene | BkF | | 2.39 | | | 18.0 | | | 40.5 | |
| Benzo[*a*]pyrene | BaP | | 0.03 | | | 0.51 | | | 0.82 | |
| Indeno[1,2,3-*cd*]pyrene | IcdP | | 0.44 | | | 6.65 | | | 8.17 | |
| Dibenz[*a,h*]anthracene | DbahA | | 0.03 | | | 0.25 | | | 0.31 | |
| **ΣTEQ *t*-PAHs** | | 0.15 | 3.22 | | 0.82 | 28.5 | | 1.74 | 55.2 | |
| Newly identified AhR agonists | | | | | | | | | | |
| Benz[*b*]anthracene | BbA | 2260 | | | 1300 | | | 4120 | | |
| 6-Methylchrysene | 6MC | | 26.5 | | | 7.8 | | | 1.4 | |
| 1,12-Dimethylbenzo[*c*]phenanthrene | DBcP | | | | | | | | 0.9 | |
| 2-Methylbenz[*a*]anthracene | 2MBaA | | 64.5 | | | | | | | |
| 1-Methylbenz[*a*]anthracene | 1MBaA | | 3.9 | | | | | | | |
| Indeno[1,2,3-*cd*]fluoranthene | IcdF | | | 14.3 | | | 7.0 | | | 7.9 |
| **ΣTEQ *n*-PAHs** | | 2260 | 94.9 | 14.3 | 1300 | 7.8 | 7.0 | 4120 | 2.3 | 7.9 |
| *Bioassay-derived TCDD-EQs (pg TCDD-EQ g$^{-1}$ dm)*[c] | | | | | | | | | | |
| **Contribution (%)** | | > 100 | > 100 | 29.2 | > 100 | 36.3 | 10.5 | > 100 | 45.6 | 20.2 |

[a] Abb: Abbreviations.

[b] Relative effect potency (ReP) values from Villeneuve et al. (2002).

[c] Data obtained from sample dose-response relationships elicited by sediment samples at six levels of dilution (Fig. S3).

mean AhR-mediated potency was greater in sediments from China (29.1%TCDD$_{max}$) than those from Korea (9.2%TCDD$_{max}$). Thirteen sites had more than 50%TCDD$_{max}$, all of which corresponded to the sites in China (Fig. 2a). In particular, sediments from sites YC6 and NT10 reached saturation efficacy ($\geq$ 100%TCDD$_{max}$) for AhR-mediated potency (Fig. S2). The regions with the greatest AhR-mediated potencies, such as Yancheng and Nantong (coastal cities of Jiangsu Province), were consistent with regions where great concentrations of PAHs in sediments were detected in previous studies (Liu et al., 2018; Yoon et al., 2020). The results of all the data confirmed that the H4IIE-*luc* responses were significantly correlated with concentrations of PAHs in sediments (Fig. 2b). Thus, the dioxin-like activity in sediments was associated with PAH concentrations in the coastal sediments of Korea and China.

In this study, EDA was performed for samples with %TCDD greater than 50% ($n$ = 13). In addition, even when AhR-mediated potency did not exceed 50%TCDD$_{max}$, sites exceeding interim sediment quality guidelines (ISQGs) of the Canadian Council of Ministers of the Environment (CCME, 2002) were selected for further fractionation ($n$ = 6), assuming that antagonistic interactions might occur (Larsson et al., 2014a) (Fig. 2b and c). For the F1–F3 of the 19 raw organic extracts, AhR-mediated potency was commonly greater in F2 (mid-polar, mean = 50%TCDD$_{max}$) and F3 (polar, mean = 38%TCDD$_{max}$) than those in F1 (non-polar, mean = 9%TCDD$_{max}$) (Fig. 2d). This result seems to be because the well-known AhR active substances, DL-PAHs and PCDD/Fs, were mainly eluted in the mid-polar fraction (Louiz et al., 2008; Hong et al., 2016b; Lee et al., 2019). In the previous study, more polar AhR agonists, including rutaecarpine, medroxyprogesterone, and canrenone, which were eluted in F3, were found in sediments (Cha et al., 2021). However, the FSA of polar contaminants in environmental samples has been successfully performed in only a few studies (Cha et al., 2021; Gallampois et al., 2015). More studies concerning unknown polar AhR agonists in sediments are needed in the future. This study focused on the identification of AhR agonists that exist in the mid-polar fraction of sediment organic extracts and are not easily metabolized. The subsequent steps focused on mid-polar AhR agonists in F2 of the top 6 sites with great AhR responses (Fig. 2e).

Of the 10 RP-HPLC fractions of F2, F2.6–F2.9 of QH6, YC6, and NT10 induced great AhR-mediated potencies (Fig. 2e). These fractions contained aromatics with 5–9 log K$_{ow}$ values (Table S1), including

traditional AhR agonists, such as benzo[*a*]anthracene (BaA), chrysene (Chr), benzo[*b*]fluoranthene (BbF), benzo[*k*]fluoranthene (BkF), BaP, indeno[1,2,3-*cd*]pyrene (IcdP), and dibenz[*a,h*]anthracene (DbahA) (Villeneuve et al., 2002; Hong et al., 2016b). This trend was similar to previous studies; great AhR-mediated potencies were found in F2.6–F2.8 of sediments from Lake Sihwa (Cha et al., 2019) and Ulsan Bay (Kim et al., 2019), Korea. The F2.9 also showed significant AhR-mediated potencies, but there were no target compounds corresponding to the fraction in the present study. Based on results of the previous study, 7–9 ring PAHs, which are superhydrophobic compounds, have been shown to have AhR activity (Thiäner et al., 2019); thus, additional confirmation was needed. To calculate potency-based TCDD-EQ concentrations, the full dose-response curves of more potent fractions were obtained (Fig. S3). These bioassay-derived TCDD-EQs were used to compare the instrument-derived TEQs in the potency balance analysis.

### 3.2. Concentrations and contribution of target PAHs

Target 15 *t*-PAHs, including known DL-PAHs, were measured in the F2.6–F2.8 of QH6, YC6, and NT10. Concentrations of fifteen *t*-PAHs in fractions ranged from 312 to 2820 ng g$^{-1}$ dm, and were detected in all sediments (Table S4). The concentration of *t*-PAH in sediment was greatest at site NT10, followed by YC6 and QH6. Concentrations of fluoranthene, pyrene, BaA, Chr, BaP, and DbahA in sediments from NT10 and YC6 exceeded the ISQGs (CCME, 2002) (Table S4). At these two sites, concentrations of PAHs were greater at F2.7 than at F2.6, with the same pattern being detected for AhR-mediated potency.

In order to determine the contributions of known AhR agonists, potency balance analyses between TCDD-EQs and TEQs were performed on fractions F2.6 and F2.7 of NT10, QH6, and YC6. Targeted DL-PAHs in fraction F2.6 explained 2.2% (mean value of three sites) of TCDD-EQs for all sediments, whereas F2.7 explained 25%. Even though fraction F2.8 exhibited the greatest potency of AhR-mediated responses, there were no targeted *t*-PAHs observed in that fraction, which means previously unidentified AhR agonists were present in fractions of sediment organic extracts. Thus, FSA was performed to identify previously unmonitored AhR agonists in fractions F2.6–F2.9 using GC-QTOFMS.
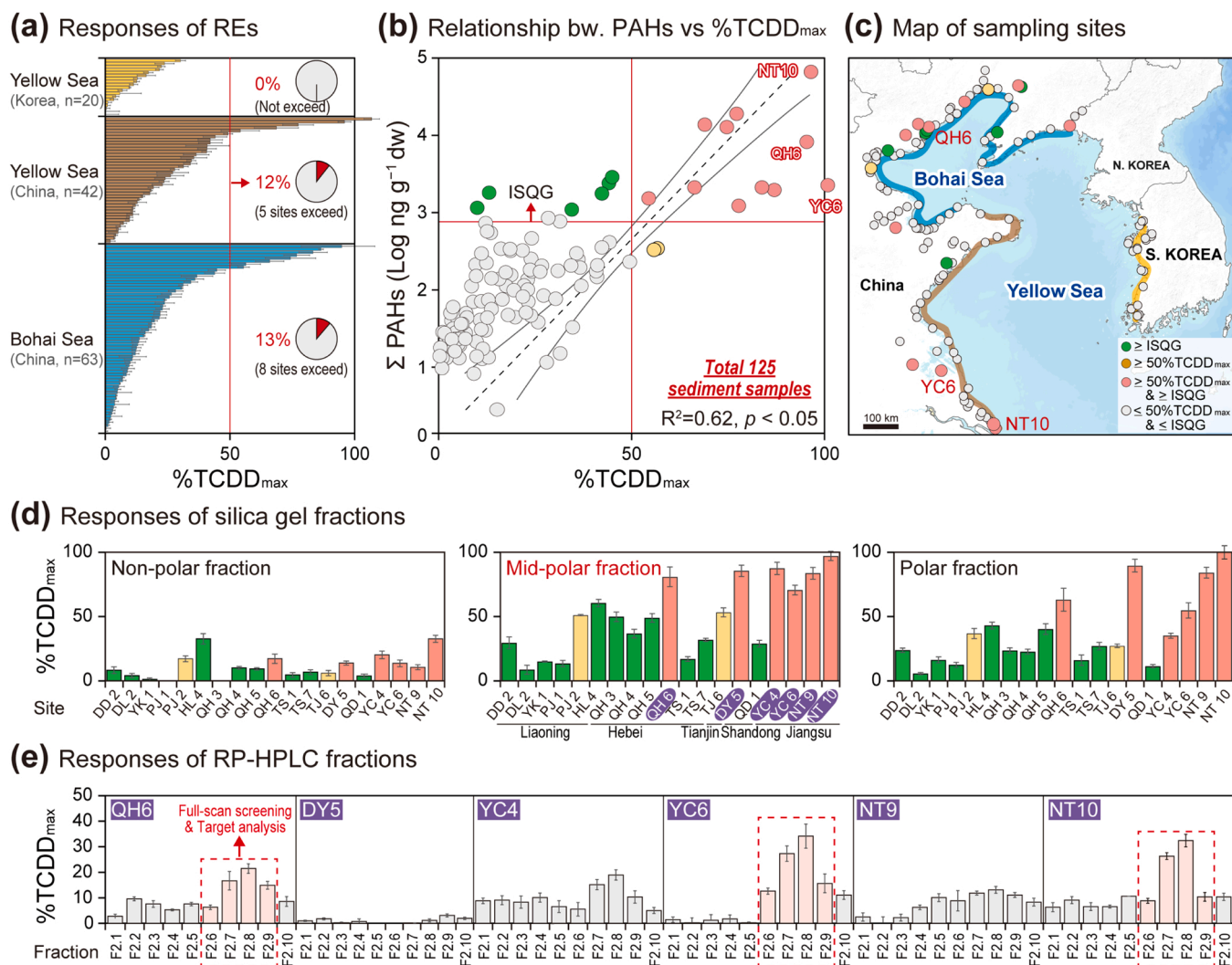
**Fig. 2.** (a) AhR-mediated potencies of raw extracts (RE) of sediments. (b) Relationship between AhR-mediated potencies and polycyclic aromatic hydrocarbons (PAHs) concentrations. (c) Map showing the sampling sites of sediments from the Yellow and Bohai Seas. Colors in circles indicate AhR-mediated potencies and concentrations of PAHs in sediments. (d) AhR-mediated potencies of silica gel fractions, and (e) RP-HPLC fractions of contaminated sediments in Yellow and Bohai Seas (Error bar: mean ± SD; $n$ = 3).

### 3.3. Full-scan screening analysis of more potent fractions

A five-step prioritization strategy was used to select candidate AhR agonists in fractions F2.6–F2.9 (Fig. 3a). GC-QTOFMS analysis revealed more than 2000 peaks in fractions F2.6–F2.9 of three sites. In the first step, > 500 compounds were matched in fractions F2.6–F2.9 by use of the NIST library (ver. 2014) (Booij et al., 2014). Next, compounds with a matching score of ≥ 70 were selected. Compounds that were present in fraction samples were selected by removing the compounds of the control and procedure blank samples. Because aromatic compounds are known to be more likely to fit the ligand-binding domain of the AhR, they were selected to move to a fourth step (Mekenyan et al., 1996). Consequently, 70 compounds in fraction F2.6 and 95 compounds in F2.7 were selected from three locations (Fig. 3a). In fractions F2.8 and F2.9, fewer than 10 compounds were selected. In the final step, AhR agonists belonging to t-PAHs and compounds that were already identified as not being AhR agonists were removed. Of the compounds analyzed at the three sites of each fraction, overlapping compounds were selected (Fig. 3a). Finally, ninety-two tentative AhR agonists were selected (Table S6). Of the 92 compounds, 13 were commercially available as authentic standards so they could be characterized for AhR-mediated responses of the H4IIE-*luc* bioassay. All candidate compounds,

including those for which AhR relative potencies could be determined empirically, were predicted AhR binding affinity using VirtualToxLab.

### 3.4. Confirmation of assay-specific relative effect potency values

AhR activities were evaluated for 13 AhR agonist candidates at both 4 and 72 h in the H4IIE-*luc* bioassay exposures (Fig. 3b). Among the 13 compounds, six compounds BaA, 6MC, DBcP, 2MBaA, 1MBaA, and IcdF exhibited detectable AhR-mediated efficacies after 4 h and 72 h exposures. Four out of six compounds reached maximum efficiency after 4 h exposure (≥ 100%BaP$_{max}$), but a lesser, but significant response after 72 h exposure. Simultaneous tests at 4 h and 72 h exposures in the H4IIE-*luc* bioassay provide useful information on the potential metabolism of AhR agonists that might occur in mixtures in samples from the environment. Relatively great AhR-mediated potency after 4 h indicates the presence of metabolizable substances in samples, while greater AhR-mediated potency after 72 h indicates the presence of non-metabolized substances, such as PCDD/Fs and coplanar-PCBs (Villeneuve et al., 2002; Louiz et al., 2008; Larsson et al., 2014b). However, due to the different standard materials (BaP for 4 h and TCDD for 72 h), the results of two bioassays could not be quantitatively compared; thus, they were compared by adjusted RLU. In the present study, newly identified AhR
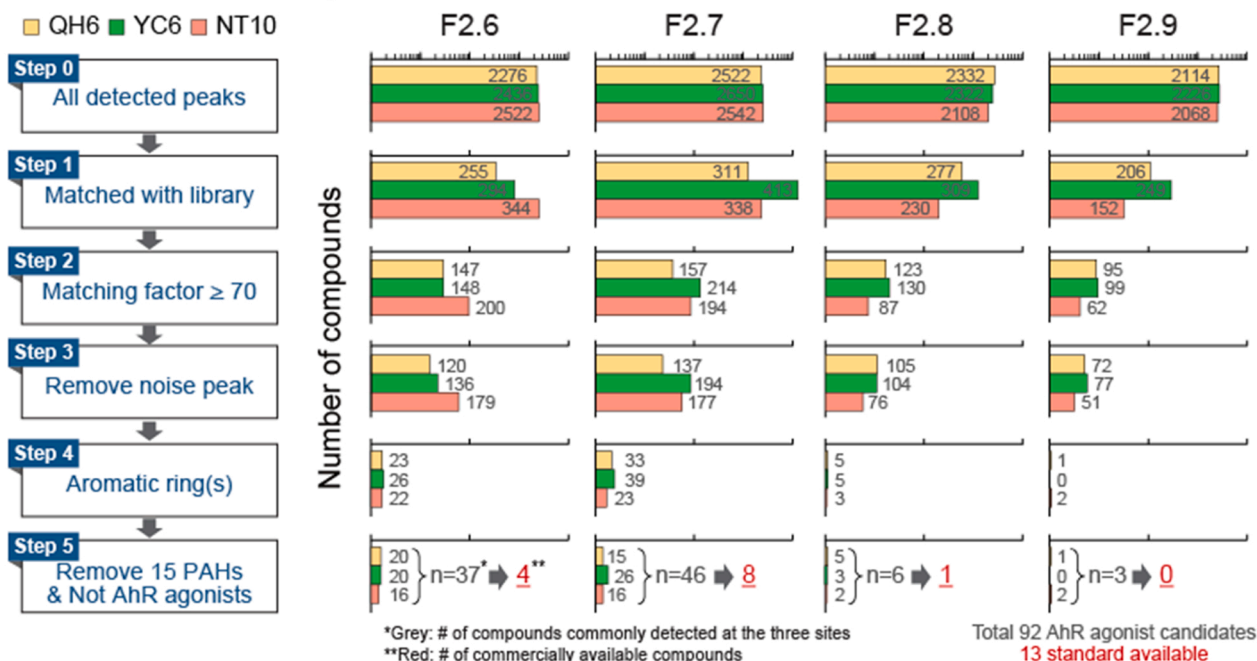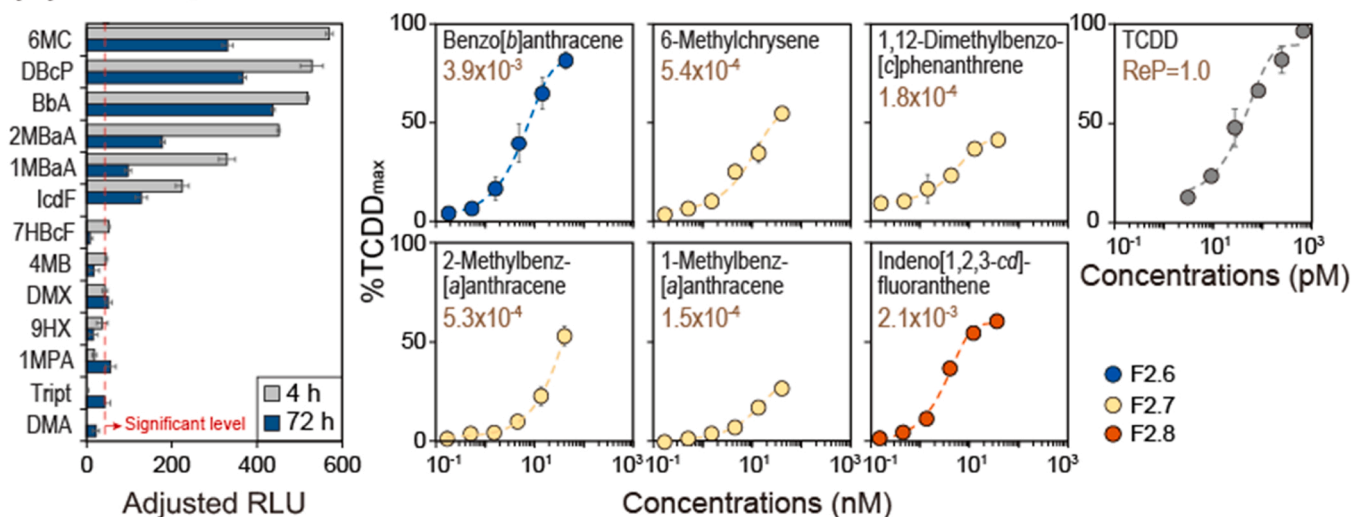
**Fig. 3.** (a) Workflow of data analysis of full-scan screening using GC-QTOFMS for selecting candidates of AhR agonists in four sub-fractions (F2.6–F2.9) from QH6, YC6, and NT10. (b) AhR-mediated potencies of thirteen tentative AhR agonists, including 6-methylchrysene (6MC), 1,12-dimethylbenzo[c]phenanthrene (DBcP), benzo[b]anthracene (BbA), 2-methylbenz[a]anthracene (2MbaA), 1-methylbenz[a]anthracene (1MBaA), indeno[1,2,3-cd]fluoranthene (IcdF), 7H-benzo[c]fluorene (7HBcF), 4-methylbenzophenone (4MB), 9,9-dimethylxanthene (DMX), 9H-xanthene (9HX), 1-methylphenanthrene (1MPA), triptycene (Tript), and 9,10-dimethyl-lanthracene (DMA) from RP-HPLC fractions (F2.6 –F2.8 of QC6, YC6, and NT10 sediment extracts) at 4 and 72 h exposure durations, and dose−response relationships for AhR-mediated potencies of newly identified AhR-active compounds in the H4IIE-*luc* bioassay (Error bar: mean ± SD. *n* = 3. ReP: relative effect potency value).

agonists exhibited relatively great AhR efficacies at both 4 h and 72 h exposures. This means that these substances retain their abilities to activate the AhR for longer times and were not readily metabolized (Lee et al., 2013).

Of the six tentative AhR agonists, four, BbA, 6MC, 2MBaA, and 1MBaA, had previously been reported to act as AhR agonists (Table 1). However, due to differences in cell line and exposure time of the bioassay, their ReP values could not be used in this study (Larsson et al., 2014). For example, *t*-PAHs can be easily degraded due to metabolism in H4IIE-*luc* cells during the longer 72 h exposure, resulting in markedly different ReP values between 4 h and 72 h (Villeneuve et al., 2002; Louiz et al., 2008; Larsson et al., 2014b). In the present study, assay-specific

ReP values for BbA, 6MC, 2MBaA, and 1MBaA were newly obtained using the H4IIE-*luc* bioassay for 72 h exposures. Compared to TCDD, ReP values of BbA, 6MC, 2MBaA, and 1MBaA were $3.9 \times 10^{-3}$, $5.4 \times 10^{-4}$, $5.3 \times 10^{-4}$, and $1.5 \times 10^{-4}$, respectively (Fig. 3b). BbA was a strong AhR agonist, which indicated that BbA is less metabolized than other AhR agonists. Compounds with a linear arrangement of fused benzene rings, such as BbA, have fewer reactive carbon atoms than compounds with a bent arrangement. Thus, they are less likely to occur degradation and transformation (Flesher and Lehner, 2016). However, it did not reach the ReP value of 10.6 compared to BaP at 4 h exposure. Since the ReP values are assay-specific, direct comparison is not appropriate. However, the newly obtained ReP values are generally

comparable to the previously reported values (Table 1). Overall, among ReP values compared to TCDD, 72 h exposure was evaluated higher than short exposure (4 h or 24 h), which is consistent with results of previous studies, in which binding occurs maximally at 72 h. It is indicated that metabolically stable compounds take a longer time to achieve AhR binding sufficiently in the H4IIE-*luc* bioassay. DBcP and IcdF are novel AhR agonists for which ReP values of $1.8 \times 10^{-4}$ and $2.1 \times 10^{-3}$ were derived for the first during the present study.

### 3.5. In silico prediction of AhR agonist candidates toxicity

Binding affinities of ligands to the AhR are correlated with potencies for activation of the AhR. To assess the AhR binding affinities of the 92 AhR agonist candidates, VirtualToxLab modeling was performed. As a result, 3 compounds showed TP values greater than 0.5 (Elevated), 26 compounds showed values greater than 0.4 and less than 0.5 (Moderate), and 30 compounds showed values greater than 0.3 and less than 0.4 (Low). Altogether, 59 of the 92 compounds were predicted to have significant and environmentally relevant AhR binding affinity (Fig. 4a and Table S6). Of the 13 compounds that were evaluated for toxicological confirmation, six were observed to have significant AhR-mediated potency with TP values of 0.4 or greater, while seven compounds observing were predicted to not have significant potency because their values were $< 0.4$. Results of tested AhR-mediated response were generally consistent with the TP values.

To more accurately consider false-positive or false-negative predictions of VirtualToxLab, in addition to the 13 AhR agonist candidates tested in this study, previous studies were reviewed, and information for 82 compounds was curated. The ratio of positive and negative agreement between the in vitro assay and in silico prediction was 66%. This means that toxicity prediction using in silico prediction was reasonably accurate with the empirically derived values. However, the statistical correlation between predicted binding affinity and experimentally determined ReP values was not significant ($R^2 = 0.04$, $p > 0.05$, Fig. 4b). Furthermore, the portion of predicting false-positive (26%) was more than the predicted false-negative (8%) (Fig. 4b). This result indicated that if the efficacy of AhR agonists is evaluated using only in silico prediction, the efficacy of the target compounds can be overestimated.

The discrepancy between experimental AhR response data and toxicity-relevant factors predicted by currently available in silico models are expected. In fact, although VirtualTox applies flexible docking combined with multi-dimensional QSAR, it is an algorithm that relies on linear regression relationships between logarithms of biotoxicity of known chemicals and their molecular structure descriptors, which are used as the training set of data. Thus, based on the QSAR model, it is predicted that the congeners in each homologue group with the same molecular mass would exhibit similar potencies for activation of the AhR, and that potency is directly proportional to molecular mass. The

results of testing with 92 AhR agonist candidate compounds in this study also showed that there was a significant positive correlation ($R^2 = 0.77$, $p < 0.01$, Fig. S4) between molecular mass and TP. However, while TP was generally directly proportional to molecular mass, it was not always the case. Overall, VirtualToxLab was useful to rapidly obtain chemical information with considerable accuracy via in silico prediction, but careful consideration of the information required and an integrated assessment of quantifying the toxic expression mechanism is needed.

### 3.6. Distribution of newly identified AhR-active compounds in sediments

GC retention time and ion fragment patterns of newly identified AhR agonists were confirmed using standard materials (Table S4). Concentrations of six newly identified AhR agonists in fractions of extracts of sediments were quantified using GC-MSD. BbA, 6MC, and IcdF were found in QH6, YC6, and NT10 (Fig. 5a). BbA occurred at the greatest concentrations, with 748 ng $g^{-1}$ dm, 412 ng $g^{-1}$ dm, and 236 ng $g^{-1}$ dm for NT10, QH6, and YC6, respectively. Concentrations of BbA in sediments from those three locations were greater than those in sediments from Yeongil Bay (188 ng $g^{-1}$ dm), which is a heavily industrialized area in South Korea (Gwak et al., 2022). The greatest concentrations of 6MC (37.3 ng $g^{-1}$ dm) and IcdP (5.84 ng $g^{-1}$ dm) were observed in sediment from QH6. Previous studies reported that the carcinogenic risk of PAHs in the sediments of Qinhuangdao exceeded the baseline with unacceptable contamination (Lin et al., 2018; Wang et al., 2020). To our knowledge, concentrations of 6MC and IcdP have not been observed in sediments from anywhere other than Qinhuangdao. The identification of new causative toxic chemicals in sediments from Qinhuangdao in this study and the results of previous studies indicate that this area will need urgent management.

DBcP (4.10 ng $g^{-1}$ dm) was only present in fraction F2.7 from NT10, while 1MBaA (20.0 ng $g^{-1}$ dm) and 2MBaA (91.0 ng $g^{-1}$ dm) were only present in fraction 2.7 from QH6 (Fig. 5a and Table S4). Contributions of *t*-PAHs and *n*-PAHs to total PAHs in QH6 and NT10 sediments exhibited the opposite trend (Fig. S5). In QH6, 77.6% of the total PAHs detected were *n*-PAHs, while *n*-PAHs of NT10 contributed only 22.7%. The contribution of *n*-PAHs in YC6 was 14%, similar to the sites of NT10, the contributions of *t*-PAHs were greater than that of *n*-PAHs. These conflicting results might be related to both regional characteristics and land-uses. Both NT10 and YC 6 are industrial areas of Jiangsu Province, while QH6 is the site of the municipal area of Hebei Province (Yoon et al., 2020). According to Yoon et al. (2020), sources of *t*-PAH as determined by positive matrix factorization (PMF), model factor 1 was greatest in QH6 and NT10, and the source was determined to be a combination of combustion of diesel fuel and gasoline (Fig. S5). In another study, vehicular emission in Qinhuangdao and petroleum combustion in Nantong were determined to be likely sources of PAHs (Lin et al., 2018; Liu et al., 2017). The source of DBcP, which is *n*-PAHs, has not been
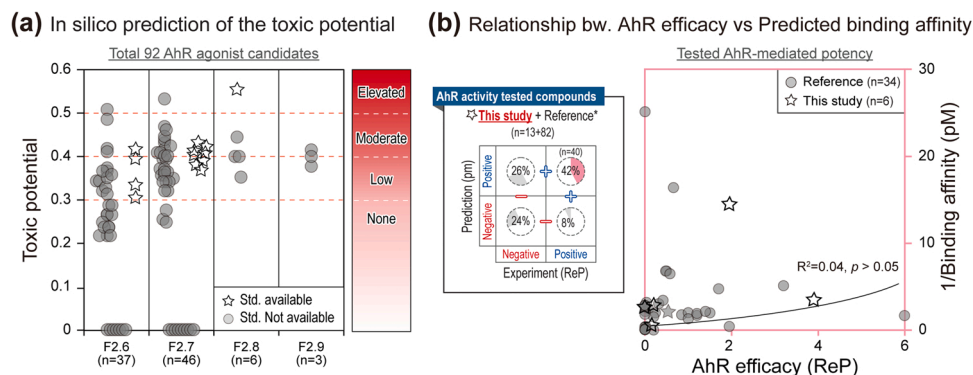


**Fig. 4.** (a) In silico prediction of the toxic potential of AhR agonist candidates in sub-fraction (F2.6–F2.9) from QH6, YC6, and NT10 using VirtualToxLab. (b) Relationship between experimental binding affinity (by use of H4IIE-*luc* bioassay) and reciprocal of calculated binding affinities by use of VirtualToxLab. Experimental data of AhR activity from this study and references (Cha et al., 2019, 2021; Gwak et al., 2022; Kim et al., 2019; Lee et al., 2020).
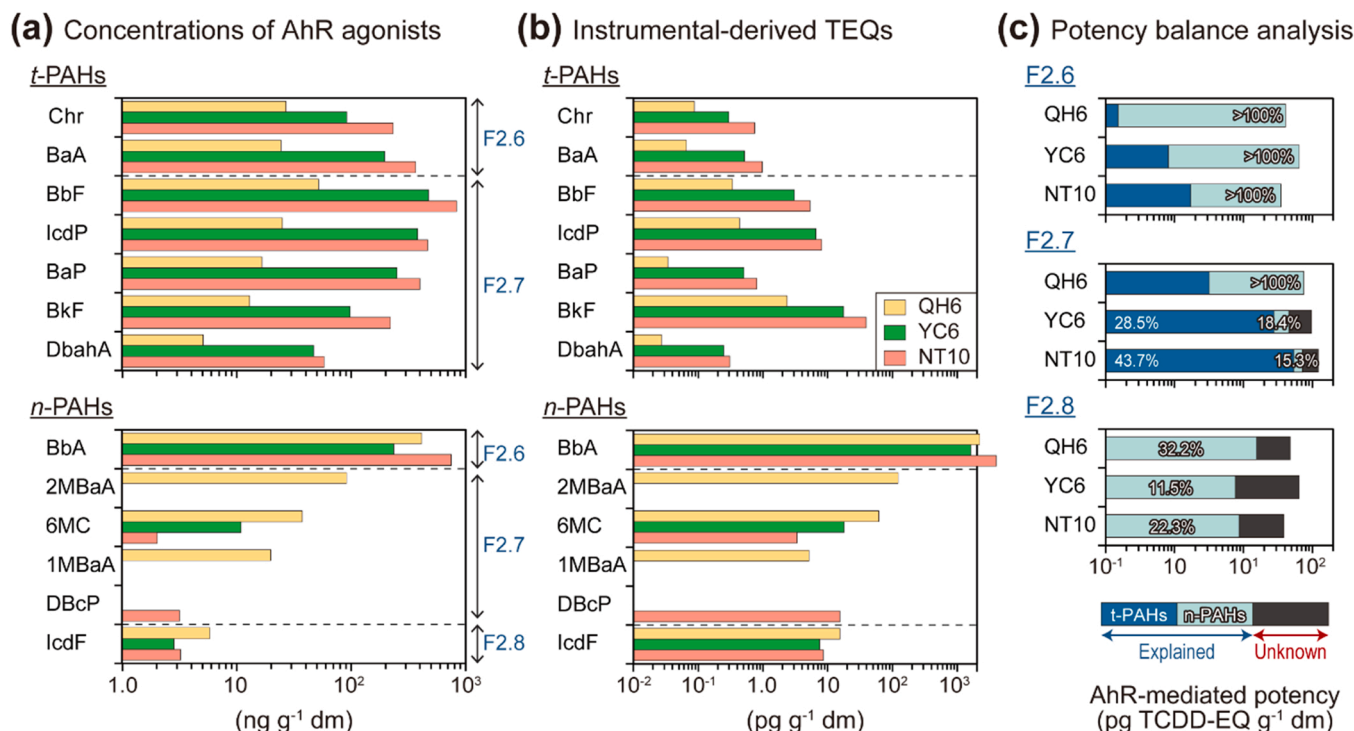
**Fig. 5.** (a) Concentrations and (b) instrument-derived toxic equivalents (TEQs) of AhR agonists, including traditional polycyclic aromatic hydrocarbons (*t*-PAHs) and newly identified PAHs (*n*-PAHs) in F2.6 to F2.8 of QH6, YC6, and NT10. (c) Potency balance analysis between bioassay-derived TCDD-EQs and instrument-derived TEQs in the RP-HPLC fractions (F2.6–F2.8) of organic extracts of sediments from QH6, YC6, and NT10 (percentage numbers in the figure indicate total contributions of newly identified AhR agonists to TCDD-EQs).

reported previously but inferred from the sources of *t*-PAHs, it is presumed to be due to petroleum-based combustion. A similar concentration of 2MBaA (42.0 ng g$^{-1}$ dm) was observed in sediments of the River Elbe, Germany (Skoczynska et al., 2013). 1MBaA and 2MBaA originate from coal combustion and charcoal smoke, respectively (Table 2) (Mumford et al., 1995; Ré-Poppi and Santiago-Silva, 2002). These compounds could be included in regular screening in the future, and their sources and fate should be delineated.

*3.7. Improved contributions of AhR agonists to total induced potency*

To determine the relative contributions of newly identified AhR agonists to unexplained portions of concentrations of TCDD-EQ, potency balance analysis was performed (Table 2). The contribution to induced potencies increased (mean = 51%) by the addition of newly identified and characterized AhR agonists (Fig. 5b). Concentrations of TCDD-EQs of fraction F2.6 of extracts of sediments from three locations were fully explained (exceeds 100%) by BbA in extracts of sediments (Fig. 5c). This result was attributed to the relatively great concentrations of BbA as well as a relatively large ReP (3.9 × 10$^{-3}$). In addition, potencies of AhR agonists assume that it acts in a strictly additive manner (Larsson et al., 2014a). However, due to possible interactions between various components of a mixture, AhR-mediated responses might be greater or lesser than predicted (Bitter et al., 2009). For example, the AhR-mediated potency of RP-HPLC fractions of F2 was simply summed and compared with the response of F2. The results of the QH6, YC6, and NT10 sites showed that the sum of the RP-HPLC fractions response was greater than the F2 response, while the response at DY5 and NT9 sites was greater in the fraction (Fig. S2b). This finding might be due to the presence of several AhR agonists of low individual activity distributed in many fractions, whereas the activity in the parent fraction was a mixture effect. Further studies are needed on the mixture toxic effects between fractions of environmental samples.

In fraction F2.7, 6MC had a relatively greater ReP value compared to

other chemicals and was the greatest contributor (Table 2). 2MBaA and 1MBaA contributed 83.3% and 5.0%, respectively to concentrations of TCDD-EQs of fraction F2.7 from QH6 (Fig. 5c and Table 1). Overall, the potency balance showed significant power to explain the greater concentrations of TCDD-EQ, when newly identified AhR agonists induced saturation efficacy (≥ 100%TCDD$_{max}$) in F2.7 from QH6 (Fig. 5c). Of the newly identified AhR agonists in F2.8, IcdF contributed significantly to TCDD-EQ in QH6 (29.2%), NT10 (20.2%), and YC6 (10.5%). This phenomenon was attributed to its relatively great ReP value, despite the compounds occurring at relatively low concentrations.

The unexplained portion might be attributed to tentative AhR agonists for which the standards were not available. For example, 2-methylchrysene (MC) is a candidate compound that is expected to act as an AhR agonist. According to Skoczynska et al. (2013), ReP of 2MC relative to chrysene was the greatest compared to that of 6MC. In addition, emerging PAHs have been reported as AhR agonists (ReP values relative to BaP), including benzo[*j*]fluoranthene (1.7), 4,5-methanochrysene (1.0), and 11 H-benzo[*a*]fluorene (1.2) (Cha et al., 2019; Kim et al., 2019). Although these substances were not detected by FSA in the current study, they have relatively great RePs; thus, their presence in trace amounts could induce significant AhR activity. Assay-specific ReP values relative to TCDD for the emerging toxic substances are needed in future research.

**4. Conclusions**

The present study is the first large-scale investigation to assess the potential toxicity of sediments along the coasts of the Yellow and Bohai Seas. Successful EDA with in silico prediction identified new AhR agonists in sediments and strongly contributed to measuring potential toxic effects. In our study, dioxin-like compounds, such as 1,12-dimethylbenzo[*c*]phenanthrene and indeno[1,2,3-*cd*]fluoranthene were first detected in sediments and exhibited binding affinity to the AhR. Additional effort is required to monitor and identify the sources of these

compounds, integrating effect-based and chemical analytical tools, as well as collecting in vitro and in vivo data of these chemicals.

## Environmental implication

This study is the first large-scale investigation to assess the potential toxicity of sediments along the coasts of the Yellow and Bohai Seas. Using advanced effect-directed analysis (EDA) with in silico prediction, hazardous substances, including 1,12-dimethylbenzo[*c*]phenanthrene and indeno[1,2,3-*cd*]fluoranthene were identified as novel AhR agonists in sediments. The novel AhR agonists showed strong AhR activity comparable to that of TCDD, and showed greater contributions to total toxicity than traditional PAHs. Combining advanced EDA with in silico approach applied in this study demonstrated the benefits of assessing the potential toxic effects of AhR agonists in contaminated sites.

## CRediT authorship contribution statement

**Junghyun Lee:** Conceptualization, Investigation, Formal analysis, Data curation, Visualization, Writing – original draft, Writing – review & editing. **Seongjin Hong:** Conceptualization, Data curation, Writing – review & editing, Project administration, Supervision. **Taewoo Kim:** Investigation, Formal analysis, Data curation. **Shin Yeong Park:** Investigation, Formal analysis. **Jihyun Cha:** Formal analysis, Data curation. **Youngnam Kim:** Formal analysis. **Jiyun Gwak:** Formal analysis. **Sunggyu Lee:** Formal analysis, Data curation. **Hyo-Bang Moon:** Formal analysis, Data curation. **Wenyou Hu:** Investigation, Project administration, Funding acquisition. **Tieyu Wang:** Investigation, Project administration, Funding acquisition. **John P. Giesy:** Conceptualization, Writing – review & editing. **Jong Seong Khim:** Investigation, Conceptualization, Writing – review & editing, Project administration, Funding acquisition, Supervision.

## Declaration of Competing Interest

The authors declare that they have no known competing financial interests or personal relationships that could have appeared to influence the work reported in this paper.

## Acknowledgments

## Appendix A. Supporting information

Supplementary data associated with this article can be found in the online version at doi:10.1016/j.jhazmat.2022.128908.

## References

Alqassim, A.Y., Wilson, M.J., Wickliffe, J.K., Pangeni, D., Overton, E.B., Miller Iii, C.A., 2019. Aryl hydrocarbon receptor signaling, toxicity, and gene expression responses to mono-methylchrysenes. Environ. Toxicol. 34, 992–1000.

Bitter, M., Hilscherova, K., Giesy, J.P., 2009. In vitro assessment of AhR-mediated activities of TCDD in mixture with humic substances. Chemosphere 76, 1505–1508.

Bláha, L., Hilscblahaherová, K., Mazurová, E., Hecker, M., Jones, P.D., Newsted, J.L., Bradley, P.W., Gracia, T., Ďuriš, Z., Horká, I., Holoubek, I., Giesy, J.P., 2006. Alteration of steroidogenesis in H295R cells by organic sediment contaminants and relationships to other endocrine disrupting effects. Environ. Int. 32, 749–757.

Bols, N.C., Schirmer, K., Joyce, E.M., Dixon, D.G., Greenberg, B.M., Whyte, J.J., 1999. Ability of polycyclic aromatic hydrocarbons to induce 7-Ethoxyresorufin-o-deethy-lase activity in a trout liver cell line. Ecotoxicol. Environ. Safe 44, 118–128.

Booij, P., Vethaak, A.D., Leonards, P.E., Sjollema, S.B., Kool, J., de Voogt, P., Lamoree, M.H., 2014. Identification of photosynthesis inhibitors of pelagic marine algae using 96-well plate microfractionation for enhanced throughput in effect-directed analysis. Environ. Sci. Technol. 48, 8003–8011.

Brack, W., 2003. Effect-directed analysis: a promising tool for the identification of organic toxicants in complex mixtures? Anal. Bioanal. Chem. 377, 397–407.

Canadian Council of Ministers of the Environment (CCME), 2002. Canadian sediment quality guidelines for the protection of aquatic life: nonylphenol and its ethoxylates. In: Canadian Environmental Quality Guidelines. CCME Winnipeg, p. 1999.

Cha, J., Hong, S., Kim, J., Lee, J., Yoon, S.J., Lee, S., Moon, H.-B., Shin, K.-H., Hur, J., Giesy, J.P., Khim, J.S., 2019. Major AhR-active chemicals in sediments of Lake Sihwa, South Korea: application of effect-directed analysis combined with full-scan screening analysis. Environ. Int. 133, 105199.

Cha, J., Hong, S., Lee, J., Gwak, J., Kim, M., Kim, T., Hur, J., Giesy, J.P., Khim, J.S., 2021. Novel polar AhR-active chemicals detected in sediments of an industrial area using effect-directed analysis based on in vitro bioassays with full-scan high resolution mass spectrometric screening. Sci. Total Environ. 779, 146566.

Chapman, P.M., 2007. Determining when contamination is pollution — weight of evidence determinations for sediments and effluents. Environ. Int. 33, 492–501.

Denison, M.S., Nagy, S.R., 2003. Activation of the aryl hydrocarbon receptor by structurally diverse exogenous and endogenous chemicals. Annu. Rev. Pharmacol. Toxicol. 43, 309–334.

Flesher, J.W., Lehner, A.F., 2016. Structure, function and carcinogenicity of metabolites of methylated and non-methylated polycyclic aromatic hydrocarbons: a comprehensive review. Toxicol. Mech. Methods 26 (3), 151–179.

Gallampois, C.M., Schymanski, E.L., Krauss, M., Ulrich, N., Bataineh, M., Brack, W., 2015. Multicriteria approach to select polyaromatic river mutagen candidates. Environ. Sci. Technol. 49, 2959–2968.

Giesy, J.P., Hilscherova, K., Jones, P.D., Kannan, K., Machala, M., 2002. Cell bioassays for detection of aryl hydrocarbon (AhR) and estrogen receptor (ER) mediated activity in environmental samples. Mar. Pollut. Bull. 45, 3–16.

Gwak, J., Cha, J., Lee, J., Kim, Y., An, S.-A., Lee, S., Moon, H.-B., Hur, J., Giesy, J.P., Hong, S., Khim, J.S., 2022. Effect-directed identification of novel aryl hydrocarbon receptor-active aromatic compounds in coastal sediments collected from a highly industrialized area. Sci. Total Environ. 803, 149969.

Hecht, S.S., Bondinell, W.E., Hoffmann, D., 1974. Chrysene and methylchrysenes: presence in tobacco smoke and carcinogenicity23. JNCI: J. Natl. Cancer Inst. 53, 1121–1133.

Hecker, M., Giesy, J.P., 2011. Effect-directed analysis of Ah-receptor mediated toxicants, mutagens and endocrine disruptors in sediments and biota. In: Brack, W. (Ed.), Effect-Directed Analysis of Complex Environmental Contamination. Vol. 15 of Handbook of Environmental Chemistry, 15. Springer, Berlin, pp. 285–313. Vol. 15 of Handbook of Environmental Chemistry.

Hernández, F., Ibáñez, M., Portolés, T., Cervera, M.I., 2015. Advancing towards universal screening for organic pollutants in waters. J. Hazard. Mater. 282, 86–95.

Hollert, H., Keiter, S., König, N., Rudolf, M., Ulrich, M., Braunbeck, T., 2003. A new sediment contact assay to assess particle-bound pollutants using zebrafish (Danio rerio) embryos. J. Soils Sed. 3, 197.

Hong, S., Giesy, J.P., Lee, J.-S., Lee, J.-H., Khim, J.S., 2016a. Effect-directed analysis: current status and future challenges. Ocean Sci. J. 51, 413–433.

Hong, S., Khim, J.S., Park, J., Kim, S., Lee, S., Choi, K., Kim, C.-S., Choi, S.-D., Park, J., Ryu, J., Jones, P.D., Giesy, J.P., 2014. Instrumental and bioanalytical measures of dioxin-like compounds and activities in sediments of the Pohang Area, Korea. Sci. Total Environ. 470–471, 1517–1525.

Hong, S., Lee, J., Lee, C., Yoon, S.J., Jeon, S., Kwon, B.-O., Lee, J.-H., Giesy, J.P., Khim, J. S., 2016b. Are styrene oligomers in coastal sediments of an industrial area aryl hydrocarbon-receptor agonists? Environ. Pollut. 213, 913–921.

Hong, S., Lee, S., Choi, K., Kim, G.B., Ha, S.Y., Kwon, B.-O., Ryu, J., Yim, U.H., Shim, W. J., Jung, J., 2015. Effect-directed analysis and mixture effects of AhR-active PAHs in crude oil and coastal sediments contaminated by the Hebei Spirit oil spill. Environ. Pollut. 199, 110–118.

Horii, Y., Khim, J.S., Higley, E.B., Giesy, J.P., Ohura, T., Kannan, K., 2009. Relative potencies of individual chlorinated and brominated polycyclic aromatic hydrocarbons for induction of aryl hydrocarbon receptor-mediated responses. Environ. Sci. Technol. 43 (6), 2159–2165.

Hwang, K., Lee, J., Kwon, I., Park, S.Y., Yoon, S.J., Lee, J., Kim, B., Kim, T., Kwon, B.-O., Hong, S., Lee, M.J., Hu, W., Wang, T., Choi, K., Ryu, J., Khim, J.S., 2021. Large-scale sediment toxicity assessment over the 15,000 km of coastline in the Yellow and Bohai seas, East Asia. Sci. Total Environ. 792, 148371.

Khim, J.S., Park, J., Song, S.J., Yoon, S.J., Noh, J., Hong, S., Kwon, B.-O., Ryu, J., Zhang, X., Wang, T., Lu, Y., Giesy, J.P., 2018. Chemical-, site-, and taxa-dependent benthic community health in coastal areas of the Bohai Sea and northern Yellow Sea: a sediment quality triad approach. Sci. Total Environ. 645, 743–752.

Kim, J., Hong, S., Cha, J., Lee, J., Kim, T., Lee, S., Moon, H.-B., Shin, K.-H., Hur, J., Lee, J.-S., Giesy, J.P., Khim, J.S., 2019. Newly identified AhR-active compounds in the sediments of an industrial area using effect-directed analysis. Environ. Sci. Technol. 53, 10043–10052.

Larsson, M., Giesy, J.P., Engwall, M., 2014a. AhR-mediated activities of polycyclic aromatic compound (PAC) mixtures are predictable by the concept of concentration addition. Environ. Int. 73, 94–103.

Larsson, M., Hagberg, J., Giesy, J.P., Engwall, M., 2014b. Time-dependent relative potency factors for polycyclic aromatic hydrocarbons and their derivatives in the H4IIE-*luc* bioassay. Environ. Toxicol. Chem. 33, 943–953.

Lee, K.T., Hong, S., Lee, J.S., Chung, K.H., Hilscherová, K., Giesy, J.P., Khim, J.S., 2013. Revised relative potency values for PCDDs, PCDFs, and non-ortho-substituted PCBs for the optimized H4IIE-*luc* in vitro bioassay. Environ. Sci. Pollut. R. 20, 8590–8599.

Lee, J., Hong, S., Kim, T., Lee, C., An, S.-A., Kwon, B.-O., Lee, S., Moon, H-B., Giesy, J.P., Khim, J.S., 2020. Multiple bioassays and targeted and nontargeted analyses to characterize potential toxicological effects associated with sediments of Masan Bay: focusing on AhR-mediated potency. Environ. Sci. Technol. 54, 4443–4454.

Lee, J., Hong, S., Kwon, B.-O., Cha, S.A., Jeong, H.-D., Chang, W.K., Ryu, J., Giesy, J.P., Khim, J.S., 2018. Integrated assessment of persistent toxic substances in sediments from Masan Bay, South Korea: comparison between 1998 and 2014. Environ. Pollut. 283, 317–325.

Lee, J., Hong, S., Yoon, S.J., Kwon, B.O., Ryu, J., Giesy, J.P., Allam, A.A., Al-Khedhairy, A.A., Khim, J.S., 2017. Long-term changes in distributions of dioxin-like and estrogenic compounds in sediments of Lake Sihwa, Korea: revisited mass balance. Chemosphere 181, 767.

Lee, J., Kim, T., Yoon, S.J., Kim, S., Lee, A.H., Kwon, B.-O., Allam, A.A., Al-khedhairy, A. A., Lee, H., Kim, J.-J., Hong, S., Khim, J.S., 2019. Multiple evaluation of the potential toxic effects of sediments and biota collected from an oil-polluted area around Abu Ali Island, Saudi Arabia, Arabian Gulf. Ecotoxicol. Environ. Safe 183, 109547.

Lin, F., Han, B., Ding, Y., Li, Q., Gao, W., Zheng, L., 2018. Distribution characteristics, sources, and ecological risk assessment of polycyclic aromatic hydrocarbons in sediments from the Qinhuangdao coastal wetland, China. Mar. Pollut. Bull. 127, 788–793.

Liu, N., Li, X., Zhang, D., Liu, Q., Xiang, L., Liu, K., Yan, D., Li, Y., 2017. Distribution, sources, and ecological risk assessment of polycyclic aromatic hydrocarbons in surface sediments from the Nantong Coast, China. Mar. Pollut. Bull. 114, 571–576.

Liu, X., Jung, D., Zhou, K., Lee, S., Noh, K., Khim, J.S., Giesy, J.P., Yim, U.H., Shim, W.J., Choi, K., 2018. Characterization of endocrine disruption potentials of coastal sediments of Taean, Korea employing H295R and MVLN assays–Reconnaissance at 5 years after Hebei Spirit oil spill. Mar. Pollut. Bull. 127, 264–272.

Louiz, I., Kinani, S., Gouze, M.E., Ben-Attia, M., Menif, D., Bouchonnet, S., Porcher, J.M., Ben-Hassine, O.K., Ait-Aissa, S., 2008. Monitoring of dioxin-like, estrogenic and anti-androgenic activities in sediments of the Bizerta lagoon (Tunisia) by means of in vitro cell-based bioassays: contribution of low concentrations of polynuclear aromatic hydrocarbons (PAHs). Sci. Total Environ. 402, 318–329.

Machala, M., Švihálková-Šindlerová, L., Pěnčíková, K., Krčmář, P., Topinka, J., Milcová, A., Nováková, Z., Kozubík, A., Vondráček, J., 2008. Effects of methylated chrysenes on AhR-dependent and -independent toxic events in rat liver epithelial cells. Toxicology 247, 93–101.

Marvanová, S., Vondráček, J., Pěnčíková, K., Trilecová, L., Krčmářř, P., Topinka, J., Nováková, Z., Milcová, A., Machala, M., 2008. Toxic effects of methylated Benz[*a*] anthracenes in liver cells. Chem. Res. Toxicol. 21, 503–512.

Mekenyan, O.G., Veith, G.D., Call, D.J., Ankley, G.T., 1996. A QSAR evaluation of Ah receptor binding of halogenated aromatic xenobiotics. Environ. Health Perspect. 104, 1302–1310.

Meng, J., Hong, S., Wang, T., Li, Q., Yoon, S.J., Lu, Y., Giesy, J.P., Khim, J.S., 2017. Traditional and new POPs in environments along the Bohai and Yellow Seas: an overview of China and South Korea. Chemosphere 169, 503–515.

Mumford, J.L., Li, X., Hu, F., Lu, X.B., Chuang, J.C., 1995. Human exposure and dosimetry of polycyclic aromatic hydrocarbons in urine from Xuan Wei, China with high lung cancer mortality associated with exposure to unvented coal smoke. Carcinogenesis 16, 3031–3036.

Murahashi, T., Watanabe, T., Kanayama, M., Kubo, T., Hirayama, T., 2007. Human aryl hydrocarbon receptor ligand activity of 31 non-substituted polycyclic aromatic hydrocarbons as soil contaminants. J. Health Sci. 53, 715–721.

Muster, W., Breidenbach, A., Fischer, H., Kirchner, S., Müller, L., Pähler, A., 2008. Computational toxicology in drug development. Drug Discov. Today 13, 303–310.

Ré-Poppi, N., Santiago-Silva, M.R., 2002. Identification of polycyclic aromatic hydrocarbons and methoxylated phenols in wood smoke emitted during production of charcoal. Chromatographia 55, 475–481.

Schymanski, E.L., Singer, H.P., Slobodnik, J., Ipolyi, I.M., Oswald, P., Krauss, M., Schulze, T., Haglund, P., Letzel, T., Grosse, S., Thomaidis, N.S., Bletsou, A., Zwiener, C., Ibanez, M., Portoles, T., de Boer, R., Reid, M.J., Onghena, M., Kunkel, U., Schulz, W., Guillon, A., Noyon, N., Leroy, G., Bados, P., Bogialli, S., Stipanicev, D., Rostkowski, P., Hollender, J., 2015. Non-target screening with high-resolution mass spectrometry: critical review using a collaborative trial on water analysis. Anal. Bioanal. Chem. 407, 6237–6255.

Skoczynska, E., Leonards, P., de Boer, J., 2013. Identification and quantification of methylated PAHs in sediment by two-dimensional gas chromatography/mass spectrometry. Anal. Methods 5, 213–218.

Takahashi, T., Takenobu, T., Takeya, J., Iwasa, Y., 2007. Ambipolar light-emitting transistors of a tetracene single crystal. Adv. Funct. Mater. 17, 1623–1628.

Thiäner, J.B., Nett, L., Zhou, S., Preibisch, Y., Hollert, H., Achten, C., 2019. Identification of 7–9 ring polycyclic aromatic hydrocarbons in coals and petrol coke using High performance liquid chromatography – Diode array detection coupled to Atmospheric pressure laser ionization – Mass spectrometry (HPLC-DAD-APLI-MS). Environ. Pollut. 252, 723–732.

Tian, K., Wu, Q., Liu, P., Hu, W., Huang, B., Shi, B., Zhou, Y., Kwon, B.-O., Choi, K., Ryu, J., Seong Khim, J., Wang, T., 2020. Ecological risk assessment of heavy metals in sediments and water from the coastal areas of the Bohai Sea and the Yellow Sea. Environ. Int. 136, 105512.

Vedani, A., Dobler, M., Smieško, M., 2012. VirtualToxLab — a platform for estimating the toxic potential of drugs, chemicals and natural products. Toxicol. Appl. Pharmacol. 261, 142–153.

Vedani, A., Dobler, M., Hu, Z., Smiesko, M., 2015. OpenVirtualToxLab — a platform for generating and exchanging in silico toxicity data. Toxicol. Lett. 232, 519–532.

Villeneuve, D., Khim, J., Kannan, K., Giesy, J., 2002. Relative potencies of individual polycyclic aromatic hydrocarbons to induce dioxin-like and estrogenic responses in three cell lines. Environ. Toxicol. 17, 128–137.

Wang, C., Zou, X., Li, Y., Zhao, Y., Song, Q., Yu, W., 2017. Pollution levels and risks of polycyclic aromatic hydrocarbons in surface sediments from two typical estuaries in China. Mar. Pollut. Bull. 114, 917–925.

Wang, P., Mi, W., Xie, Z., Tang, J., Apel, C., Joerss, H., Ebinghaus, R., Zhang, Q., 2020. Overall comparison and source identification of PAHs in the sediments of European Baltic and North Seas, Chinese Bohai and Yellow Seas. Sci. Total Environ. 737, 139535.

Xiao, H., Krauss, M., Floehr, T., Yan, Y., Bahlmann, A., Eichbaum, K., Brinkmann, M., Zhang, X., Yuan, X., Brack, W., Hollert, H., 2016. Effect-directed analysis of aryl hydrocarbon receptor agonists in sediments from the Three Gorges Reservoir, China. Environ. Sci. Technol. 50, 11319–11328.

Yang, L., Zhou, Y., Shi, B., Meng, J., He, B., Yang, H., Yoon, S.J., Kim, T., Kwon, B.-O., Khim, J.S., Wang, T., 2020. Anthropogenic impacts on the contamination of pharmaceuticals and personal care products (PPCPs) in the coastal environments of the Yellow and Bohai seas. Environ. Int. 135, 105306.

Yoon, S.J., Hong, S., Kim, S., Lee, J., Kim, T., Kim, B., Kwon, B.-O., Zhou, Y., Shi, B., Liu, P., Hu, W., Huang, B., Wang, T., Khim, J.S., 2020. Large-scale monitoring and ecological risk assessment of persistent toxic substances in riverine, estuarine, and coastal sediments of the Yellow and Bohai seas. Environ. Int. 137, 105517.

Zhang, F., Wang, H., Zhang, L., Zhang, J., Fan, R., Yu, C., Wang, W., Guo, Y., 2014. Suspected-target pesticide screening using gas chromatography-quadrupole time-of-flight mass spectrometry with high resolution deconvolution and retention index/mass spectrum library. Talanta 128, 156–163.

# Identification of AhR agonists in sediments of the Bohai and Yellow Seas using advanced effect-directed analysis and in silico prediction

Junghyun Lee, Seongjin Hong[*], Taewoo Kim, Shin Yeong Park, Jihyun Cha, Youngnam Kim,

Jiyun Gwak, Sunggyu Lee, Hyo-Bang Moon, Wenyou Hu, Tieyu Wang, John P. Giesy,

Jong Seong Khim[*]

**This file includes:**

Number of pages: 16

Number of Supplementary Tables: 7, Tables S1 to S7

Number of Supplementary Figures: 5, Figs. S1 to S5

References

**\*Corresponding authors.**

*E-mail addresses*: hongseongjin@cnu.ac.kr (S. Hong); jskocean@snu.ac.kr (J.S. Khim).

# Supplementary Tables

**Table S1.** Instrumental conditions of reverse phase(RP)-HPLC for the fractionation of silica gel column fractions (Hong et al., 2016).

| **Instrument** | Agilent 1260 HPLC system (Preparative scale) |
|---|---|
| | 1260 Multiple wavelength detector |
| **Column** | PrepHT XDB-C18 reverse phase column (250 mm × 21.2 mm × 7 μm) |
| **Mobile phase** | Water (A):MeoH (B) (40:60, v/v), Isocratic elution |
| **Injection volume** | 1 mL |
| **Flow rate** | 10 mL min$^{-1}$ |
| **Mobile phase gradient** | |

| Time | Solvent | |
|---|---|---|
| (min.) | A | B |
| 0 | 40 | 60 |
| 40 | 0 | 100 |
| 65 | 0 | 100 |
| 66 | 0 | 60 |
| 70 | 40 | 60 |

**Test standards**

34 polychlorinated biphenyls
16 polycyclic aromatic hydrocarbons
7 alkylphenols
5 phthalates

**Fractions collected times**

| RP-HPLC Sub-fraction | Starting –End sampling time (min.) | Volume (mL) | Log $K_{OW}$ |
|---|---|---|---|
| 1 | 3.11 – 6.35 | 38 | < 1 |
| 2 | 6.35 – 12.83 | 65 | 1 – 2 |
| 3 | 12.83 – 19.32 | 65 | 2 – 3 |
| 4 | 19.32 – 25.80 | 65 | 3 – 4 |
| 5 | 25.80 – 32.29 | 65 | 4 – 5 |
| 6 | 32.29 – 38.78 | 65 | 5 – 6 |
| 7 | 38.78 – 45.26 | 65 | 6 – 7 |
| 8 | 45.26 – 51.70 | 65 | 7 – 8 |
| 9 | 51.70 – 58.23 | 65 | 8 – 9 |
| 10 | 58.23 – 64.72 | 65 | > 9 |

**Table S2.** Description of the experimental conditions for H4IIE-*luc in vitro* bioassay.

| Cell line | H4IIE-*luc* | |
|---|---|---|
| | Rat hepatoma cells that were stably transfected with a luciferase reporter gene | |
| Endpoint | AhR-mediated potencies | |
| Medium | Dulbecco's Modified Eagle's Medium (Sigma, St.Louis, MO) supplemented with 10% fetal bovine serum | |
| Test chamber | 96-well culture plates with 5%$CO_2$ atmosphere | |
| Solvent carrier | 0.1% DMSO | |
| Temperature (°C) | 37 | |
| Initial concentrations | $7.0 \times 10^4$ cells mL$^{-1}$ | |
| Test duration (h) | 4 | 72 |
| Positive control | Benzo[*a*]pyrene | 2,3,7,8-tetrachlorodibenzo-*p*-dioxin (2,3,7,8-TCDD) |
| Initial concentration | 50 nM | 729 pM |
| Replicates | 3 | |

**Table S3.** Instrumental conditions of GC-MSD for detecting PAHs.
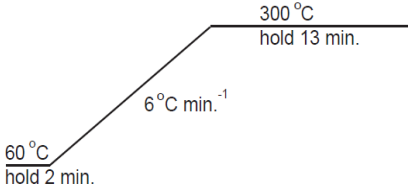
| Instrument | GC: Agilent Technologies 7890B |
| --- | --- |
| | MSD: Agilent Technologies 5977A |
| **Column** | DB-5MS (30 m × 0.25 mm i.d. × 0.25 μm film) |
| **Carrier gas** | He |
| **Flow rate** | 1.0 mL min.$^{-1}$ |
| **Inlet temperature** | 300 °C |
| **Injection volume** | 1 μL (Spitless mode) |
| **Mass range** | 50−600 $m/z$ |
| **Ion source temperature** | 230 °C |
| **Ionization mode** | EI mode (70 eV) |
| **Oven temperature** | |

300 °C
hold 13 min.

6 °C min.$^{-1}$

60 °C
hold 2 min.

| **Recoveries of surrogate standards** | **Surrogate standards** | **Surrogate recovery (%, mean ± SD)** |
| --- | --- | --- |
| | Acenaphthene-d10 | 82 ± 12 |
| | Phenanthrene-d10 | 86 ± 9 |
| | Chrysene-d12 | 91 ± 7 |
| | Perylene-d12 | 90 ± 11 |

**Table S4.** Abbreviations, concentrations, and method detection limit for targeted and newly identified PAHs in the RP-HPLC fraction samples (F2.6, F2.7, and F2.8) of organic extracts from NT10, QH6, and YC6 sediment using GC-MS.

| Compounds | Abb.[a] | Method detection limit ($ng\ g^{-1}$) | GC RT[b] (min) | Mass Fragmentations (m/z) | NT10 F2.6 | F2.7 | F2.8 | QH6 F2.6 ($ng\ g^{-1}$) | F2.7 | F2.8 | YC6 F2.6 | F2.7 | F2.8 |
|---|---|---|---|---|---|---|---|---|---|---|---|---|---|
| *Traditional-PAHs (ISQG)[c]* | | | | | | | | | | | | | |
| Acenaphthene (6.71) | Ace | 1.1 | | | 1.75 | <LOD[d] | | 2.10 | <LOD | | 3.36 | <LOD | |
| Acenaphthylene (5.87) | Acl | 1.7 | | | 1.82 | <LOD | | 1.84 | <LOD | | 1.93 | <LOD | |
| Fluorene (21.2) | Flu | 1.1 | | | 1.67 | <LOD | | 1.34 | <LOD | | 3.16 | <LOD | |
| Phenanthrene (86.7) | Phe | 3.1 | | | 18.5 | <LOD | | 3.46 | <LOD | | 8.87 | <LOD | |
| Anthracene (46.9) | Ant | 3.9 | | | 36.6 | <LOD | | 14.8 | <LOD | | 28.3 | <LOD | |
| Fluoranthene (113) | Fl | 4.1 | | | 1050[e] | <LOD | | 151 | <LOD | | 300 | <LOD | |
| Pyrene (153) | Py | 4.7 | | | 770 | <LOD | | 108 | <LOD | | 241 | <LOD | |
| Benzo[a]anthracene (74.8) | BaA* | 15.1 | | | 366 | <LOD | | 24.4 | <LOD | | 196 | <LOD | |
| Chrysene (108) | Chr* | 4.8 | | | 233 | <LOD | | 26.9 | <LOD | | 91.7 | <LOD | |
| Benzo[b]fluoranthene | BbF* | 2.6 | | | <LOD | 834 | | <LOD | 52.0 | | <LOD | 473 | |
| Benzo[k]fluoranthene | BkF* | 3.2 | | | <LOD | 220 | | <LOD | 13.0 | | <LOD | 97.9 | |
| Benzo[a]pyrene (88.8) | BaP* | 1.1 | | | <LOD | 399 | | <LOD | 16.6 | | <LOD | 251 | |
| Indeno[1,2,3-cd]pyrene | IcdP* | 4.1 | | | <LOD | 467 | | <LOD | 25.1 | | <LOD | 381 | |
| Dibenz[a,h]anthracene (6.22) | DbahA* | 2.2 | | | <LOD | 58.1 | | <LOD | 5.1 | | <LOD | 47.1 | |
| Benzo[g,h,i]perylene | BghiP | 3.8 | | | <LOD | 344 | | <LOD | 21.9 | | <LOD | 308 | |
| **Sum of *t*-PAHs** | | | | | **1390** | **2820** | | **475** | **312** | | **541** | **1810** | |
| *Newly identified AhR agonists** | | | | | | | | | | | | | |
| Benz[b]anthracene | BbA | 2.00 | 32.4 | *228*[f], 226, 227[g] | 748 | <LOD | <LOD | 412 | <LOD | <LOD | 236 | <LOD | <LOD |
| 6-methylchrysene | 6MC | 0.92 | 34.6 | *242*, 241, 227 | <LOD | 2.02 | <LOD | <LOD | 37.3 | <LOD | <LOD | 11.0 | <LOD |
| 2-methylbenz[a]anthracene | 2MBaA | 1.95 | 34.7 | *242*, 241, 239 | <LOD | <LOD | <LOD | <LOD | 91.0 | <LOD | <LOD | <LOD | <LOD |
| 1-methylbenz[a]anthracene | 1MBaA | 8.27 | 35.6 | *242*, 241, 239 | <LOD | <LOD | <LOD | <LOD | 20.0 | <LOD | <LOD | <LOD | <LOD |
| 1,12-mimethylbenzo[c]phenanthrene | DBcP | 1.19 | 22.4 | *256, 176, 88* | <LOD | 4.10 | <LOD | <LOD | <LOD | <LOD | <LOD | <LOD | <LOD |
| Indeno[1,2,3-cd]fluoranthene | IcdF | 1.49 | 53.3 | *276*, 277, 275 | <LOD | <LOD | 3.24 | <LOD | <LOD | 5.84 | <LOD | <LOD | 2.84 |
| **Sum of *n*-PAHs** | | | | | **748** | **6.12** | **3.24** | **412** | **148** | **5.84** | **236** | **11.0** | **2.84** |

[a] Abb.: Abbreviations.
[b] GC RT: Gas chromatography retention time.
[c] ISQG: Interim sediment quality guidelines (ISQGs) recommended by the Canadian Council of Ministers of the Environment (CCME, 2002).
[d] < LOD: Below detection limits.
[e] Shade indicates concentrations that exceed ISQG values.
[f] Quantification ion.
[g] Confirmation ions.
* AhR agonist compounds confirmed in this study.

**Table S5.** Instrumental conditions of GC-QTOFMS for full-scan screening analysis.

| | |
|---|---|
| **Instrument** | GC: Agilent Technologies 7890B<br>QTOFMS: Agilent Technologies 7200 |
| **Samples** | F2.6, F2.7, F2.8 and F2.9 RP-HPLC fractions from Site NT10, QH6, and YC6 |
| **Column** | DB-5MS UI (30 m × 0.25 mm i.d. × 0.25 μm film) |
| **Carrier gas** | He |
| **Flow rate** | 1.2 mL min.$^{-1}$ |
| **Injection volume** | 2 μL |
| **Mass range** | 50–800 $m/z$ |
| **Ion source temperature** | 230 °C |
| **Ionization mode** | EI mode (70 eV) |
| **Tuning condition** | - Instruments are tuned prior to use each day batches are initiated.<br>- Tuned with a compound of known mass spectrum; perfluorotributyl-amine (PFTBA)<br>- Ions from the PFTBA spectrum for its tuning: $m/z$ 68.9947, 130.9915, 218.9851, 413.9770, 463.9738 and 501.9706<br>- Mass accuracy and correct mass errors to within 5 ppm |
| **Software** | Qualitative analysis B.07.01<br>MassHunter Quantitative analysis<br>Unknown analysis<br>NIST Library (ver. 2014) |

**Table S6.** Relative effect potency values for newly identified AhR agonists compared to the potency of TCDD in the H4IIE-*luc* bioassay.

| Compounds | Maximum concentration [a] | %TCDD$_{max}$ | Slope | Relative potency$_{20\text{-}50\text{-}80}$ [b] | |
|---|---|---|---|---|---|
| | | | | ReP$_{50}$ | ReP$_{20\text{-}80}$ |
| TCDD | 729 pM | 100 | 37 | 1.0 | 1.0–1.0 |
| BbA | 44 nM | 82 | 35 | $3.9 \times 10^{-3}$ | $4.3 \times 10^{-3} - 3.6 \times 10^{-3}$ |
| 6MC | 41 nM | 55 | 25 | $5.4 \times 10^{-4}$ | $6.4 \times 10^{-4} - 3.0 \times 10^{-4}$ |
| DBcP | 39 nM | 41 | 16 | NQ [c] | $1.8 \times 10^{-4} - $ NQ |
| 2MBaA | 41 nM | 53 | 33 | $5.3 \times 10^{-4}$ | $6.5 \times 10^{-4} - 4.4 \times 10^{-4}$ |
| 1MBaA | 41 nM | 26 | 11 | NQ | $1.5 \times 10^{-4} - $ NQ |
| IcdF | 36 nM | 60 | 33 | $2.1 \times 10^{-3}$ | $2.6 \times 10^{-3} - 1.7 \times 10^{-3}$ |

[a] 0.1% dosing concentration.

[b] ReP20-50-80: RePs reported as the range of ReP values generated from multiple point values over a response range from 20 to 50 to 80%TCDD$_{max}$.

[c] NQ: Not quantifiable for ReP calculation, dose–response relationship insufficient for estimation.

**Table S7.** List of candidates for AhR agonists in the fraction samples (F2.6, F2.7, F2.8, and F2.9) of silica gel column fractions (F2) from sediment samples (NT10, QH6, and YC6) using GC-QTOFMS. AhR binding potencies and potential toxicity of compounds were measured using VirtualToxLab modeling.

| No | Fractions and candidate substances | CAS# | QH6 | YC6 | NT10 | Formula | MW | Match factor | AhR potency | Toxic Potential[a] |
|---|---|---|---|---|---|---|---|---|---|---|
| **F2.6** | | | | | | | | | | |
| 1 | 1,1'-Biphenyl, 3-methyl- | 643-93-6 | | √ | | C13H12 | 168 | 82.8 | 3.63e-06 | 0.32 |
| 2 | 1,1'-Biphenyl, 4,4'-dimethyl- | 613-33-2 | √ | | | C14H14 | 182 | 94.4 | 3.41e-06 | 0.32 |
| 3 | 1,1-Dichloro-2,2-bis(p-chlorophenyl)ethane | 72-54-8 | | | √ | C14H10Cl4 | 318 | 79.3 | 2.68e-08 | 0.51 |
| 4 | 1-Naphthyl phenylethynyl sulfone | 2000503-48-6 | √ | | | C18H12O2S | 292 | 82 | -[b] | - |
| 5 | 2-Methylnaphtho[2,1-b]furan | 2000150-17-4 | √ | √ | | C13H10O | 182 | 82.3 | 3.83e-05 | 0.22 |
| 6 | 4,5-dihydro-pyrene | 6628-98-4 | | √ | | C16H12 | 204 | 96.1 | 4.94e-06 | 0.30 |
| 7 | 4,6,8-Trimethylazulene | 941-81-1 | √ | | | C13H14 | 170 | 75.9 | 2.90e-05 | 0.23 |
| 8 | 4-Deuteriocyclopenta[c,d]pyrene | 2000286-14-2 | √ | | | C18H9D | 226 | 81.3 | - | - |
| 9 | 4-Phenyl-3,1-benzoxathiin | 2000292-33-6 | √ | | | C14H12OS | 228 | 85.4 | - | - |
| 10 | 5H-Indeno[1,2-b]pyridin-5-amine, 4-methyl- | 58787-09-0 | √ | | | C13H12N2 | 196 | 80.8 | - | - |
| 11 | 5-Methylene-10-hydroxamino-10,11-dihydro-5H-dibenzo[a,d]cycloheptene | 70449-85-3 | √ | | | C16H15NO | 237 | 70.3 | - | - |
| 12 | 9-Ethyl-10-methylanthracene | 19713-49-6 | √ | | | C17H16 | 220 | 82.9 | 1.53e-06 | 0.35 |
| 13 | 9H-Fluorene-4-thiol | 2000195-47-2 | √ | | | C13H10S | 198 | 87.7 | 1.92e-05 | 0.25 |
| 14 | 9H-Fluorene, 9-methyl- | 2523-37-7 | √ | √ | | C14H12 | 180 | 88.0 | 3.94e-06 | 0.31 |
| 15 | 9H-Thioxanthene | 261-31-4 | | | √ | C13H10S | 198 | 76.2 | 1.29e-06 | 0.36 |
| 16 | 9H-xanthene* | 92-83-1 | √ | | | C13H10O | 182 | 89.1 | 1.12e-05 | 0.27 |
| 17 | Benzo[a]azulene | 246-02-6 | √ | | | C14H10 | 178 | 92.9 | 2.54e-06 | 0.33 |
| 18 | Benzo[b]anthracene * | 92-24-0 | √ | √ | √ | C18H12 | 228 | 86.2 | 2.89e-07 | 0.42 |
| 19 | Benzene, 1-methyl-2-(phenylmethyl)- | 713-36-0 | √ | √ | √ | C14H14 | 182 | 95.7 | 1.66e-06 | 0.35 |
| 20 | Benzene, 1-methyl-4-(phenylmethyl)- | 620-83-7 | √ | √ | √ | C14H14 | 182 | 92.7 | 2.13e-06 | 0.34 |
| 21 | Bicyclo[4.1.0]hepta-1,3,5-triene, 7-(7H-benzocyclohepten-7-ylidene)- | 109685-02-1 | √ | | √ | C18H12 | 228 | 90.8 | -[a] | - |
| 22 | (E)-1,4-Diphenyl-1-buten-3-yne | 13141-45-2 | √ | | | C16H12 | 204 | 85.5 | 5.60e-08 | 0.48 |
| 23 | 4-Methylbenzophenone * | 134-84-9 | | | √ | C14H12O | 196 | 87.2 | 5.67e-07 | 0.39 |
| 24 | Naphthalene, 1-ethyl- | 1127-76-0 | | √ | | C12H12 | 156 | 91.9 | 1.86e-05 | 0.25 |
| 25 | Naphthalene, 2-phenyl- | 612-94-2 | √ | √ | √ | C16H12 | 204 | 88.6 | 3.13e-07 | 0.42 |
| 26 | Naphthalene, 2-methyl-1-(1-methylethyl)- | 32114-79-7 | √ | | | C14H16 | 184 | 77.2 | - | - |
| 27 | Naphthalene, 1-(1-methylethyl)- | 6158-45-8 | √ | | | C13H14 | 170 | 82.7 | 7.08e-06 | 0.29 |
| 28 | Naphthalene, 1,2-dimethyl- | 573-98-8 | √ | | √ | C12H12 | 156 | 80.4 | 3.27e-05 | 0.23 |
| 29 | Naphthalene, 1,3-dimethyl- | 575-41-7 | √ | | | C12H12 | 156 | 85.6 | 3.77e-05 | 0.22 |
| 30 | Naphthalene, 1,6-dimethyl- | 575-43-9 | | | √ | C12H12 | 156 | 93.3 | 3.01e-05 | 0.23 |
| 31 | Naphthalene, 1,7-dimethyl- | 575-37-1 | √ | √ | | C12H12 | 156 | 83.2 | 3.03e-05 | 0.23 |
| 32 | Naphthalene, 1,8-dimethyl- | 569-41-5 | √ | √ | √ | C12H12 | 156 | 91.6 | 4.16e-05 | 0.22 |
| 33 | Naphthalene, 1,6,7-trimethyl- | 2245-38-7 | √ | √ | √ | C13H14 | 170 | 84.5 | 1.89e-05 | 0.25 |
| 34 | Naphthalene, 2,3,6-trimethyl- | 829-26-5 | √ | | | C13H14 | 170 | 92.4 | 1.53e-05 | 0.26 |

**Table S7.** (continued).

| No | Fractions and candidate substances | CAS# | QH6 | YC6 | NT10 | Formula | MW | Match factor | AhR potency | Toxic Potential[a] |
|---|---|---|---|---|---|---|---|---|---|---|
| 35 | Octocrylene | 6197-30-4 | √ | | √ | C24H27NO2 | 361 | 85.3 | 3.69e-07 | 0.41 |
| 36 | Phenaleno[1,9-bc]thiophene | 79965-99-4 | | √ | √ | C14H8S | 208 | 80.9 | 1.51e-05 | 0.26 |
| 37 | Phenanthrene, 1-methyl-* | 832-69-9 | √ | | | C15H12 | 192 | 90.3 | 4.26e-06 | 0.31 |
| | *Total* | | 20 | 20 | 16 | | | | | |
| **F2.7** | | | | | | | | | | |
| 1 | 1,1,4,5,6-Pentamethyl-2,3-dihydro-1H-indene | 16204-67-4 | | √ | | C14H20 | 188 | 86.1 | 2.15e-05 | 0.24 |
| 2 | 1-(o-Biphenylyl)-2-phenylethyne | 2000379-00-6 | | √ | | C20H14 | 254 | 85.3 | 1.80e-07 | 0.44 |
| 3 | 1-Ethyl-4,5,8-trimethylnaphthalene | 71185-34-7 | | √ | | C15H18 | 198 | 91.9 | 1.17e-05 | 0.27 |
| 4 | 1-Propene, 3-(2-cyclopentenyl)-2-methyl-1,1-diphenyl- | 2000447-13-1 | √ | √ | | C21H22 | 274 | 84.8 | 4.68e-08 | 0.49 |
| 5 | 2,2',5,5'-Tetramethal-1.1'-biphenyl | 3075-84-1 | √ | √ | √ | C16H18 | 210 | 94.6 | 6.67e-07 | 0.39 |
| 6 | 2,3,9-Trichlorodibenzofuran | 58802-18-9 | √ | | | C12H5Cl3O | 270 | 74.6 | 6.22e-07 | 0.39 |
| 7 | 2,4-Diphenyl-4-methyl-2(E)-pentene | 22768-22-5 | √ | √ | √ | C18H20 | 236 | 86.3 | 2.75e-07 | 0.42 |
| 8 | 2,4,5,7-Tetramethylphenanthrene | 2000273-93-6 | √ | √ | | C17H18 | 222 | 82.8 | 2.11e-06 | 0.34 |
| 9 | 2,4,6,8-Tetramethylazulene | 2000157-19-2 | | √ | | C14H16 | 184 | 92.4 | 1.86e-05 | 0.25 |
| 10 | 2-Methylchrysene | 3351-32-4 | √ | √ | | C19H14 | 242 | 90.9 | 4.54e-07 | 0.36 |
| 11 | 3-(p-Chlorophenyl)-1,2-dihydroisoquinolin-1(2H)-one | 2000381-75-0 | | √ | | C15H10ClNO | 255 | 77.1 | - | - |
| 12 | 3,5,7-Tris(trimethylsiloxy)-2-[3,4-di(trimethylsiloxy)phenyl]-4H-1-benzopyran-4-one | 4067-66-7 | √ | | | C30H50O7Si5 | 662 | 71.7 | - | - |
| 13 | 4H-Benz[de]anthracene, 5,6-dihydro- | 4389-09-7 | | | √ | C17H14 | 218 | 86.2 | 1.33e-06 | 0.36 |
| 14 | 5,5-Dimethyl-5H-dibenzo[B,D]silole | 13688-68-1 | √ | | | C14H14Si | 210 | 73.8 | - | - |
| 15 | 5,6-Dihydrochrysene | 2091-92-1 | | √ | | C18H14 | 230 | 88.7 | 4.60e-07 | 0.40 |
| 16 | 7-Ethyl-1-methylphenanthrene | 2000265-85-3 | √ | | | C17H16 | 220 | 88.7 | 1.28e-06 | 0.36 |
| 17 | 7H-Benzo[c]fluorene * | 205-12-9 | √ | | | C17H12 | 216 | 72.5 | 7.58e-07 | 0.38 |
| 18 | 9,10-Dimethylanthracene * | 781-43-1 | √ | √ | | C16H14 | 206 | 83.0 | 3.27e-06 | 0.32 |
| 19 | 9-propyl-anthracene | 0-00-0 | | √ | | C17H16 | 220 | 77.5 | 1.42e-07 | 0.45 |
| 20 | 13H-Dibenzo[a,h]fluorene | 239-85-0 | | | √ | C21H14 | 266 | 76.2 | 9.41e-08 | 0.46 |
| 21 | anti-9-Methyl-1,6-methanofluorene | 65150-18-7 | | √ | | C15H14 | 194 | 86.4 | - | - |
| 22 | Azulene, 1,4-dimethyl-7-(1-methylethyl)- | 489-84-9 | | √ | | C15H18 | 198 | 87.5 | 3.04e-06 | 0.32 |
| 23 | Benz[a]anthracene, 8,12-dimethyl- | 20627-31-0 | √ | | | C20H16 | 256 | 85.8 | 4.26e-07 | 0.40 |
| 24 | Benz[a]anthracene, 1-methyl- * | 2498-77-3 | √ | | | C19H14 | 242 | 71.5 | 3.67e-07 | 0.41 |
| 25 | Benz[a]anthracene, 2-methyl- * | 2498-76-2 | √ | | | C19H14 | 242 | 89.0 | 3.37e-07 | 0.41 |
| 26 | Benz[a]anthracene, 12-ethyl- | 18868-66-1 | | √ | | C20H16 | 256 | 74.7 | 2.18e-07 | 0.43 |
| 27 | Benzo[c]phenanthrene, 1,12-dimethyl-* | 4076-43-1 | | | √ | C20H16 | 256 | 80.7 | 1.83e-06 | 0.43 |
| 28 | Benz[e]acephenanthrylene | 205-99-2 | | √ | | C20H12 | 252 | 97.3 | 1.51e-07 | 0.44 |
| 29 | Chrysene, 6-methyl- * | 1705-85-7 | √ | √ | | C19H14 | 242 | 84.7 | 4.56e-07 | 0.40 |
| 30 | Clofenotane | 50-29-3 | | | √ | C14H9Cl5 | 352 | 93.9 | 1.28e-08 | 0.54 |
| 31 | Cyclohexene, 1-(2-methyl-2-cyclopenten-1-yl)- | 58543-96-7 | | √ | √ | C12H18 | 162 | 85.9 | - | - |
| 32 | Cyclopenta(cd)pyrene, 3,4-dihydro- | 25732-74-5 | | √ | | C18H12 | 228 | 94.3 | 2.57e-06 | 0.33 |
| 33 | Dibenzo[b,kl]xanthene | 2000425-29-6 | | | √ | C20H12O | 268 | 84.8 | - | - |
| 34 | (E)-1-Methyl-2-styrylbenzene | 74685-42-0 | | √ | | C15H14 | 194 | 93.0 | 3.61e-07 | 0.41 |

**Table S7.** (continued).

| No | Fractions and candidate substances | CAS# | QH6 | YC6 | NT10 | Formula | MW | Match factor | AhR potency | Toxic Potential[a] |
|---|---|---|---|---|---|---|---|---|---|---|
| 35 | (E)-1,5-Diphenyl-1-penten-4-yne | 2000258-94-1 | | √ | √ | C17H14 | 218 | 85.8 | - | - |
| 36 | Naphtho[2,1,8,7-klmn]xanthene | 191-37-7 | | | √ | C18H10O | 242 | 86.0 | 1.47e-06 | 0.35 |
| 37 | Naphthalene, 1-methyl-2-(1-methylethyl)- | 61994-26-1 | | √ | | C14H16 | 184 | 96.5 | 4.74e-06 | 0.31 |
| 38 | Naphthalene, 1-methyl-7-(1-methylethyl)- | 490-65-3 | | √ | | C14H16 | 184 | 95.5 | 2.12e-06 | 0.34 |
| 39 | Naphthalene, 1,6-dimethyl-4-(1-methylethyl)- | 483-78-3 | √ | | | C15H18 | 198 | 95.8 | 3.56e-06 | 0.32 |
| 40 | O,P'-DDT | 789-02-6 | | | √ | C14H9Cl5 | 352 | 79.4 | 5.93e-08 | 0.48 |
| 41 | Pallescensin E | 56881-47-1 | | | √ | C15H16O | 212 | 72.2 | 1.50e-06 | 0.35 |
| 42 | P,P'-DDE | 2000585-42-0 | √ | | | C14H10Cl4 | 318 | 70.2 | - | - |
| 43 | Retene | 483-65-8 | √ | | | C18H18 | 234 | 89.5 | - | - |
| 44 | Tribenzo[b,d,f]oxepine | 2000345-33-6 | | | √ | C18H12O | 244 | 82.6 | 3.37e-07 | 0.41 |
| 45 | Triptycene * | 477-75-8 | | √ | | C20H14 | 254 | 89.4 | 9.64e-07 | 0.37 |
| 46 | Xanthene, 9,9-dimethyl- * | 19814-75-6 | | √ | | C15H14O | 210 | 84.2 | 3.63e-07 | 0.31 |
| | *Total* | | **15** | **26** | **16** | | | | | |
| **F2.8** | | | | | | | | | | |
| 1 | 3,3,7-trimethyl-1,2,3,4-tetrahydro-chrysene | 2000447-14-4 | √ | √ | | C21H22 | 274 | 91.3 | 4.53e-07 | 0.40 |
| 2 | 3,4,7 - trimethyl - 1,2,3,4 - tetrahydro - chrysene | 2000447-12-8 | √ | | | C21H22 | 274 | 70.9 | 4.39e-07 | 0.40 |
| 3 | 8-hydroxy indeno[1,2,3-cd]pyrene | 99520-58-8 | | | | C22H12O | 292 | 75.8 | 9.96e-08 | 0.46 |
| 4 | Indeno[1,2,3-cd]fluoranthene * | 193-43-1 | √ | √ | √ | C22H12 | 276 | 93.7 | 6.92e-08 | 0.48 |
| 5 | p-Dicyclohexylbenzene | 1087-02-1 | √ | √ | √ | C18H26 | 242 | 874.7 | 9.77e-09 | 0.56 |
| 6 | Traseolide | 68140-48-7 | √ | | | C18H26O | 258 | 72.1 | 1.18e-06 | 0.36 |
| | *Total* | | **5** | **3** | **2** | | | | | |
| **F2.9** | | | | | | | | | | |
| 1 | 3,3,7,12a-tetramethyl-1,2,3,4,4a,11,12,12a-octahydro-chrysene | 2000506-42-4 | | | √ | C22H28 | 292 | 75.8 | 1.01e-06 | 0.37 |
| 2 | 4b,8-Dimethyl-2-isopropylphenanthrene, 4b,5,6,7,8,8a,9,10-octahydro- | 2000387-71-2 | | | √ | C19H28 | 256 | 75.3 | 2.57e-07 | 0.42 |
| 3 | Dehydroabietan | 19407-28-4 | √ | | | C20H30 | 270 | 71.6 | 3.78e-07 | 0.40 |
| | *Total* | | **1** | **0** | **2** | | | | | |

[a] Toxic potential (TP): TP < 0.3 showed in blue (none binding), 0.3 ≤ TP < 0.4 showed in green (low binding), 0.4 ≤ TP < 0.5 showed in orange (moderate binding), and 0.5 ≤ TP < 0.6 showed in red (elevated binding).

[b] -: not available.
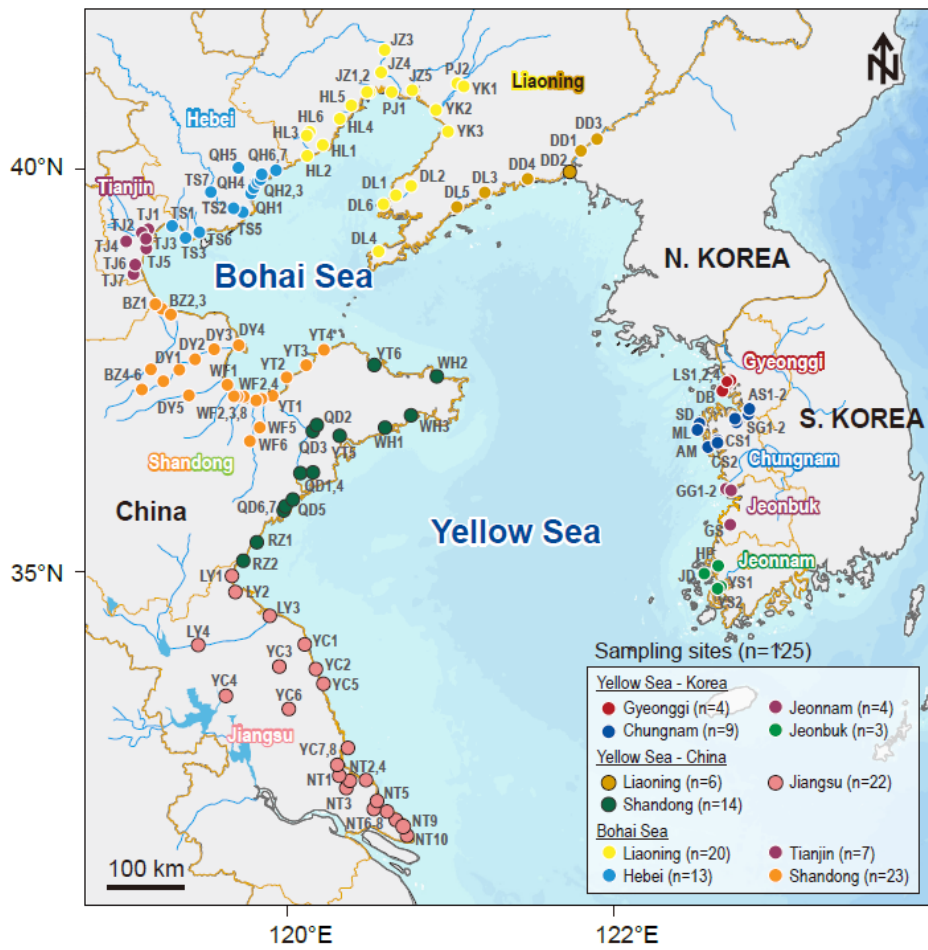
* Available for authentic standards.

**Supplementary Figures**



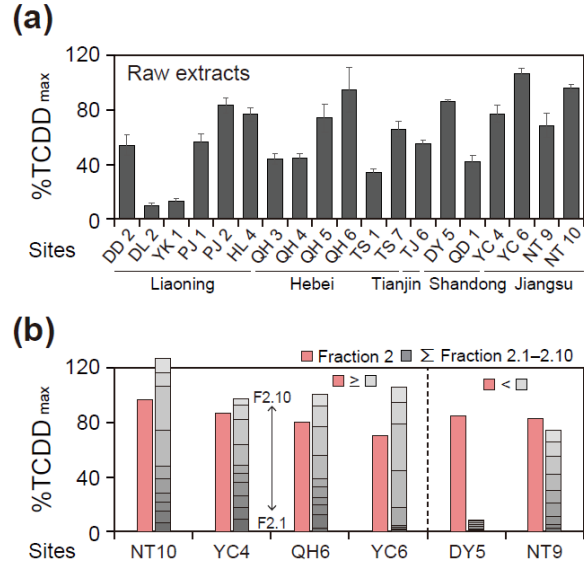**Fig. S1**. Sampling sites of surface sediments in the Yellow and Bohai Seas.

**Fig. S2**. **(a)** AhR-mediated potencies of raw extracts (REs) of contaminated sediments of Yellow and Bohai Seas (Bar with the mean ± SD; *n* = 3). **(b)** AhR-mediated potencies of more potent fraction (F2) and sum of measured AhR-mediated potency values of subfractions (F2.1–F2.10).
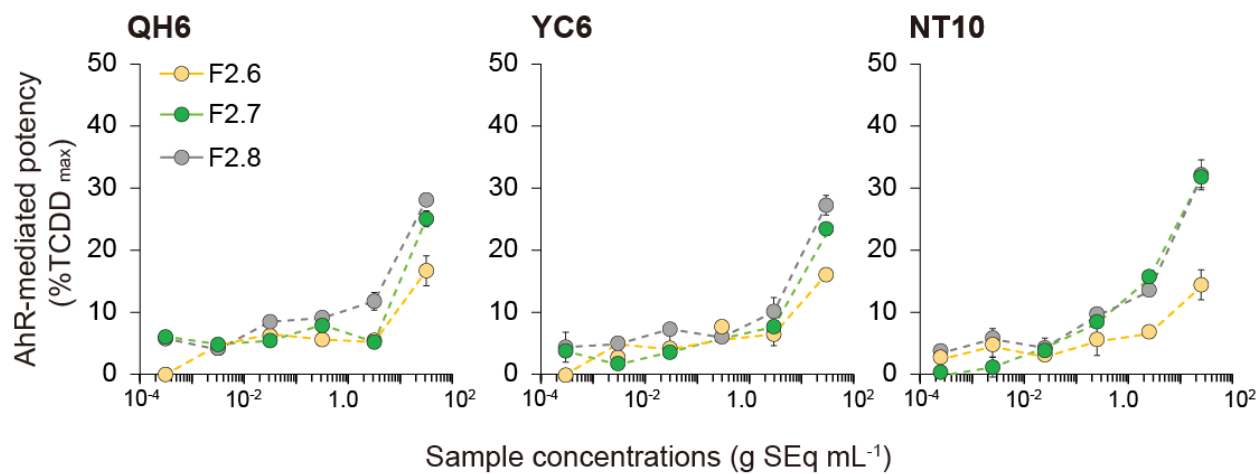
**Fig. S3.** Dose-response curves for the AhR-mediated potency of RP-HPLC fractions (F2.6 –F2.8 of NT10, QC6, and YC6 sediment extracts) from the Yellow and Bohai Seas (SEq: sediment equivalents; Error bar: mean ± SD; $n = 3$). Curves of F2.9 were not included in the Figure because the EC50 values could not be obtained.
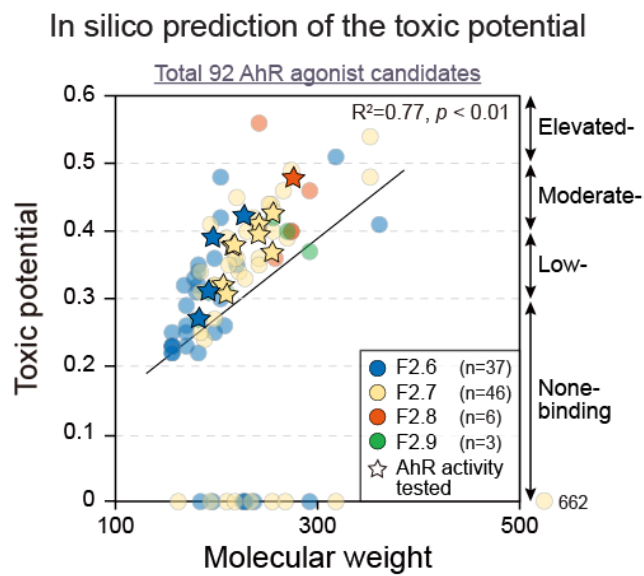
**Fig. S4.** In silico prediction of toxic potency and molecular masses of tested chemicals.
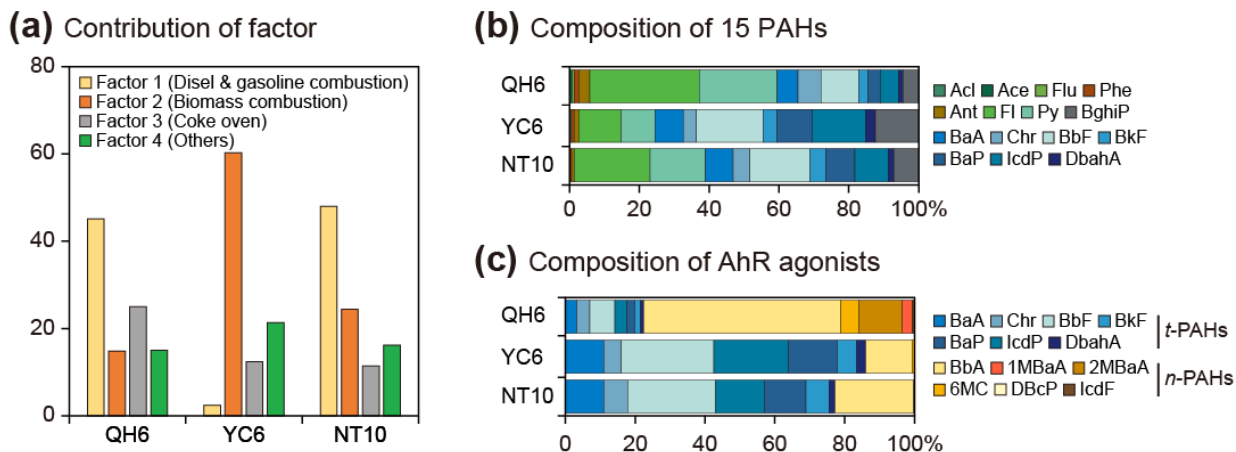
**Fig. S5. (a)** Contribution of factor scores resulting from the PMF model for predicting sources of PAHs in F2 fraction from the sediments of the QH6 (Factor 1 dominant), YC6 (Factor 2 dominant), and NT10 (Factors 1 dominant) [Data from Yoon et al. (2020)]. Compositions of **(b)** 15 polycyclic aromatic hydrocarbons (PAHs), and **(c)** AhR agonists (traditional PAHs (t-PAHs) and newly identified PAHs (n-PAHs) in RP-HPLC fraction in the sediments of QH6, YC6, and NT10.

**References**

Canadian Council of Ministers of the Environment (CCME), Canadian sediment quality
    guidelines for the protection of aquatic life summary tables. CCME: Winnipeg, MB,
    2002.

Hong, S., Lee, J., Lee, C., Yoon, S. J., Jeon, S., Kwon, B.O., Lee, J.H., Giesy, J.P., Khim, J.S.,
    2016. Are styrene oligomers in coastal sediments of an industrial area aryl hydrocarbon-
    receptor agonists? Environ. Pollut. 213, 913–921.

Villeneuve, D.L., Khim, J.S., Kannan, K., Giesy, J.P., 2002. Relative potencies of individual
    polycyclic aromatic hydrocarbons to induce dioxinlike and estrogenic responses in three cell
    lines. Environ. Toxicol. 17, 128–137.

Yoon, S.J., Hong, S., Kim, S., Lee, J., Kim, T., Kim, B., Kwon, B.-O., Zhou, Y., Shi, B., Liu, P.,
    Hu, W., Huang, B., Wang, T., Khim, J.S., 2020. Large-scale monitoring and ecological risk
    assessment of persistent toxic substances in riverine, estuarine, and coastal sediments of the
    Yellow and Bohai seas. Environ. Int. 137, 105517.